Author's personal copy

Acknowledgement

We are indebted to Professor Takashi Obinata, Dr. Hiroshi Abe, and Dr. Naruki Sato of Chiba University, Japan, for the ultracentrifugal treatment in sample preparation for two-dimensional gel electrophoresis. This work was supported in part by Grant-in-Aid for Scientific Research of Japan and Selective Research Fund of Tokyo Metropolitan University (to N. I.).

References

[1] P.J. Horner, T.D. Palmer, New roles for astrocytes: the nightlife of an 'astrocyte', La vida loca! Trends Neurosci. 26 (2003) 597–603.
[2] G.E. Barreto, J. Gonzalez, Y. Torres, L. Morales, Astrocytic–neuronal crosstalk: implications for neuroprotection from brain injury, Neurosci. Res. 71 (2011) 107–113.
[3] H.U. Lee, Y. Yamazaki, K.F. Tanaka, K. Furuya, M. Sokabe, H. Hida, K. Takao, T. Miyakawa, S. Fujii, K. Ikenaka, Increased astrocytic ATP release results in enhanced excitability of the hippocampus, Glia (Sep. 27 2012), http://dx.doi.org/10.1002/glia.22427.
[4] R.S. Ashton, A. Conway, C. Pangarkar, J. Bergen, K.-I. Lim, P. Shah, M. Bissell, D.V. Schaffer, Astrocytes regulate adult hippocampal neurogenesis through ephrin-B signaling, Nat. Neurosci. 15 (2012) 1399–1408.
[5] F. Doetsch, I. Caille, D.A. Lim, J.M. Garcia-Verdugo, A. Alvarez-Buylla, Subventricular zone astrocytes are neural stem cells in the adult mammalian brain, Cell 97 (1999) 703–716.
[6] A. Kriegstein, A. Alvarez-Buylla, The glial nature of embryonic and adult neural stem cells, Annu. Rev. Neurosci. 32 (2009) 149–184.
[7] H. Mi, B.A. Barres, Purification and characterization of astrocyte precursor cells in the developing rat optic nerve, J. Neurosci. 19 (1999) 1049–1061.
[8] K.J.N. Seidman, A.L. Teng, R. Rosenkopf, P. Spilotro, J.A. Weyhenmeyer, Isolation, cloning and characterization of a putative type-1 astrocyte cell line, Brain Res. 753 (1997) 18–26.
[9] T. Nakayama, T. Momoki-Soga, N. Inoue, Astrocyte-derived factors instruct differentiation of embryonic stem cells into neurons, Neurosci. Res. 46 (2003) 241–249.
[10] T. Nakayama, T. Momoki-Soga, K. Yamaguchi, N. Inoue, Efficient production of neural stem cells and neurons from embryonic stem cells, Neuroreport 15 (2004) 487–491.
[11] T. Nakayama, T. Sai, M. Otsu, T. Momoki-Soga, N. Inoue, Astrocytogenesis of embryonic stem-cell-derived neural stem cells: default differentiation, Neuroreport 17 (2006) 1519–1523.
[12] T. Nakayama, N. Inoue, Neural stem sphere method: Induction of neural stem cells and neurons by astrocyte derived factors in ES cells in vitro, Methods Mol. Biol. 330 (2006) 1–13.
[13] M. Otsu, T. Sai, T. Nakayama, K. Murakami, N. Inoue, Uni-directional differentiation of mouse embryonic stem cells into neurons by the neural stem sphere method, Neurosci. Res. 69 (2011) 314–321.
[14] S. Muramatsu, T. Okuno, Y. Suzuki, T. Nakayama, T. Kakiuchi, N. Takino, A. Iida, F. Ono, K. Terao, N. Inoue, I. Nakano, Y. Kondo, H. Tsukada, Multitracer assessment of dopamine function after transplantation of embryonic stem cell-derived neural stem cell in a primate model of Parkinson's disease, Synapse 63 (2009) 541–548.
[15] T. Okuno, T. Nakayama, N. Konishi, H. Michibata, K. Wakimoto, Y. Suzuki, S. Nito, T. Inaba, I. Nakano, S. Muramatsu, M. Takano, Y. Kondo, N. Inoue, Selfcontained induction of neurons from human embryonic stem cells, PLoS One 4 (2009) e6318.
[16] H. Suemori, T. Tada, R. Torii, Y. Hosoi, K. Kobayashi, H. Imahie, Y. Kondo, A. Iritani, N. Nakatsuji, Establishment of embryonic stem cell lines from cynomolgus monkey blastocysts produced by IVF or ICSI, Dev. Dyn. 222 (2001) 273–279.
[17] T. Toda, N. Kimura, Standardization of protocol for Immobiline 2-D PAGE and construction of 2-D PAGE protein database on World Wide Web home page, Jpn. J. Electrophor. 41 (1997) 13–20.
[18] K. Akama, T. Horikoshi, T. Nakayama, M. Otsu, N. Imaizumi, M. Nakamura, T. Toda, M. Inuma, H. Hirano, Y. Kondo, Y. Suzuki, N. Inoue, Proteomic characterization during neural differentiation from monkey embryonic stem cells into neurons in vitro, Biochim. Biophys. Acta 1814 (2011) 265–276.
[19] S. Patrakitkomjorn, D. Kobayashi, T. Morikawa, M. Morifuji-Wilson, N. Tsubota, A. Irie, T. Ozawa, M. Aoki, N. Arimura, K. Kaibuchi, H. Saya, N. Araki, Neurofibromatosis type 1 (NF1) tumor suppressor, neurofibromin, regulates the neuronal differentiation of PC12 cells via its associating protein, CRMP-2, J. Biol. Chem. 283 (2008) 9399–9413.
[20] S.A. Ross, P.J. McCaffery, U.C. Drager, L.M. De Luca, Retinoids in embryonal development, Physiol. Rev. 80 (2000) 1021–1054.
[21] N. Arimura, K. Kaibuchi, Neuronal polarity: from extracellular signals to intracellular mechanisms, Nat. Rev. Neurosci. 8 (2007) 194–205.
[22] M.H. Maurer Jr., R.E. Feldmann, C.D. Futterer, J. Butlin, W. Kuschinsky, Comprehensive proteome expression profiling of undifferentiated versus differentiated neural stem cells from adult rat hippocampus, Neurochem. Res. 29 (2004) 1129–1144.
[23] R. Hoffrogge, S. Mikkat, C. Scharf, S. Beyer, H. Christoph, J. Pahnke, E. Mix, M. Berth, A. Uhrmacher, I.Z. Zubrzycki, E. Miljan, U. Völker, A. Rolfs, 2-DE proteome analysis of a proliferating and differentiating human neuronal stem cell line (ReNcell VM), Proteomics 6 (2006) 1833–1847.
[24] J.I. Chae, J. Kim, S.M. Woo, H.W. Han, Y.K. Cho, K.-B. Oh, K.H. Nam, Y.K. Kang, Cytoskeleton-associated proteins are enriched in human embryonic-stem cell-derived neuroectodermal spheres, Proteomics 9 (2009) 1128–1141.
[25] K. Akama, R. Tatsuno, M. Otsu, T. Horikoshi, T. Nakayama, M. Nakamura, T. Toda, N. Inoue, Proteomic identification of differentially expressed genes in mouse neural stem cells and neurons differentiated from embryonic stem cells in vitro, Biochim. Biophys. Acta 1784 (2008) 773–782.
[26] T. Sasaki, Y. Takai, The Rho small G protein family-Rho GDI system as a temporal and spatial determinant for cytoskeletal control, Biochem. Biophys. Res. Commun. 245 (1998) 641–645.
[27] Y. Arai, N. Funatsu, K. Numayama-Tsuruta, T. Nomura, S. Nakamura, N. Osumi, Role of Fabp7, a downstream gene of Pax6, in the maintenance of neuroepithelial cells during early embryonic development of the rat cortex, J. Neurosci. 25 (2005) 9752–9761.
[28] T.E. Anthony, C. Klein, G. Fishell, N. Heintz, Radial glia serve as neuronal Progenitors on all regions of the central nervous system, Neuron 41 (2004) 881–890.
[29] Y. Owada, T. Yoshimoto, H. Kondo, Spatio-temporally differential expression of gene for three members of fatty acid binding proteins in developing and mature rat brains, J. Chem. Neuroanat. 12 (1996) 113–122.
[30] Y. Owada, S.A. Abdelwahab, N. Kitanaka, H. Sakagami, H. Takano, Y. Sugitani, M. Sugawara, H. Kawashima, Y. Kiso, J.I. Mobarakeh, K. Yanai, K. Kaneko, H. Sasaki, H. Kato, S. Saino-Saito, N. Matsumoto, N. Akaike, T. Noda, H. Kondo, Altered emotional behavioral responses in mice lacking brain-type fatty acid-binding protein gene, Eur. J. Neurosci. 24 (2006) 175–187.
[31] A. Watanabe, T. Toyota, Y. Owada, T. Hayashi, Y. Iwayama, M. Matsumata, Y. Ishitsuka, A. Nakaya, M. Maekawa, T. Ohnishi, R. Arai, K. Sakurai, K. Yamada, H. Kondo, K. Hashimoto, N. Osumi, T. Yoshikawa, Fabp7 maps to a quantitative trait locus for a schizophrenia endophenotype, PLoS Biol. 5 (e297) (2007) 1–15.
[32] J.E. McConnell, J.F. Armstrong, P.E. Hodges, J.B. Bard, The mouse 14–3–3 epsilon isoform, a kinase regulator whose expression pattern is modulated in mesenchyme and neuronal differentiation, Dev. Biol. 169 (1995) 218–228.
[33] X. Gao, H.Y. Tian, L. Liu, M.L. Yu, N.H. Jing, F.K. Zhao, Comparative proteomic analysis of proteins involved in cell aggregation during neural differentiation of P19 mouse embryonic carcinoma cells, J. Proteome Res. 8 (2009) 1765–1781.
[34] D. Wang, L. Gao, Proteomic analysis of neural differentiation of mouse embryonic stem cells, Proteomics 5 (2005) 4414–4426.
[35] Y. Takamori, Y. Tamura, Y. Kataoka, Y. Cui, S. Seo, T. Kanazawa, K. Kurokawa, H. Yamada, Differential expression of nuclear lamin, the major component of nuclear lamina, during neurogenesis in two germinal regions of adult rat brain, Eur. J. Neurosci. 25 (2007) 1653–1662.
[36] K. Nakata, H. Ujike, A. Sakai, M. Takaki, T. Imamura, Y. Tanaka, S. Kuroda, The human dihydropyrimidinase-related protein 2 gene on chromosome 8p21 is associated with paranoid-type schizophrenia, Biol. Psychiatry 53 (2003) 571–576.
[37] A.R. Cole, W. Noble, L. van Aalten, F. Plattner, R. Meimaridou, D. Hogan, M. Taylor, J. LaFrancois, F. Gunn-Moore, A. Verkhratsky, S. Oddo, F. LaFerla, K.P. Giese, K.T. Dineley, K. Duff, J.C. Richardson, S.D. Yan, D.P. Hanger, S.M. Allan, C. Sutherland, Collapsin response mediator protein-2 hyperphosphorylation is an early event in Alzheimer's disease progression, J. Neurochem. 103 (2007) 1132–1144.
[38] T. Kimura, H. Watanabe, A. Iwamatsu, K. Kaibuchi, Tubulin and CRMP-2 complex is transported via Kinesin-1, J. Neurochem. 93 (2005) 1371–1382.
[39] T. Yoshimura, Y. Kawano, N. Arimura, S. Kawabata, A. Kikuchi, K. Kaibuchi, GSK-3beta regulates phosphorylation of CRMP-2 and neuronal polarity, Cell 120 (2005) 137–149.
[40] J. Lew, Q.Q. Huang, Z. Qi, R.J. Winkfein, R. Aebersold, T. Hunt, J.H. Wang, A brain-specific activator of cyclin-dependent kinase 5, Nature 371 (1994) 423–426.
[41] M. Nikolic, H. Dudek, Y.T. Kwon, Y.F. Ramos, L.H. Tsai, The cdk5/p35 kinase Is essential for neurite outgrowth during neuronal differentiation, Genes Dev. 10 (1996) 816–825.
[42] T. Chae, Y.T. Kwon, R. Bronson, P. Dikkes, E. Li, L.H. Tsai, Mice lacking p35, a neuronal specific activator of Cdk5, display cortical lamination defects, seizures, and adult lethality, Neuron 18 (1997) 29–42.
[43] A.R. Cole, F. Causeret, G. Yadirgi, C.J. Hastie, H. McLauchlan, E.J. McManus, F. Hernández, B.J. Eickholt, M. Nikolic, C. Sutherland, Distinct priming kinases contribute to differential regulation of collapsing response mediator proteins by glycogen synthase kinase-3 in vivo, J. Biol. Chem. 281 (2006) 16591–16598.
[44] K. Niederreither, V. Subbarayan, P. Dolle, P. Chambon, Embryonic retinoic acid synthesis is essential for early mouse post-implantation development, Nat. Genet. 21 (1999) 444–448.
[45] A. Perz-Edwards, N.L. Hardison, E. Linney, Retinoic acid-mediated gene expression in transgenic reporter zebrafish, Dev. Biol. 229 (2001) 89–101.
[46] A. Budhu, R. Gillilan, N. Noy, Localization of the RAR interaction domain of cellular retinoic acid binding protein-II, J. Mol. Biol. 305 (2001) 939–949.
[47] D. Dong, S.E. Ruuska, D.J. Levinthal, N. Noy, Distinct roles for cellular retinoic acid binding proteins I and II in regulating signaling by retinoic acid, J. Biol. Chem. 274 (1999) 23695–23698.
[48] R. Chu, Y. Lin, S. Rao, J. Reddy, Cloning and identification of rat deoxyuridine triphosphatase as an inhibitor of peroxisome proliferator-activated receptor, J. Biol. Chem. 271 (1996) 27670–27676.
[49] S. Abu-Abed, P. Dolle, D. Metzger, B. Beckett, P. Chambon, M. Petkovich, The Retinoic acid-metabolizing enzyme, CYP26A1, is essential for normal hindbrain patterning, vertebral identity, and development of posterior structures, Genes Dev. 15 (2001) 226–240.
[50] V. Azais-Braesco, G. Pasca, Vitamin A in pregnancy: requirements and safety limits, Am. J. Clin. Nutr. 71 (2000) 1325S–1333S.
[51] P. Fernando, S. Brunette, L.A. Megeney, Neural stem cell differentiation is dependent upon endogenous caspase 3 activity, FASEB J. 19 (2005) 1671–1673.
[52] R. Kageyama, T. Ohtsuka, T. Kobayashi, Roles of Hes genes in neural development, Dev. Growth Differ. 50 (2008) S97–S103.
[53] Y. Koyama, Y. Yoshioka, T. Matsuda, A. Baba, Focal adhesion kinase is required for endothelin-induced cell cycle progression of cultured astrocytes, Glia 43 (2003) 185–189.

Journal of proteome research

Article

pubs.acs.org/jpr

Secretome-Based Identification of TFPI2, A Novel Serum Biomarker for Detection of Ovarian Clear Cell Adenocarcinoma

Noriaki Arakawa,[†,‡,*] Etsuko Miyagi,[§] Ayako Nomura,[‡] Erina Morita,[†] Yoko Ino,[‡] Norihisa Ohtake,[∥] Yohei Miyagi,[⊥] Fumiki Hirahara,[§] and Hisashi Hirano[†,‡,*]

[†]Department of Medical Life Science, Graduate School of Medical Life Science, Yokohama City University, Yokohama, Kanagawa, Japan

[‡]Advanced Medical Research Center, Yokohama City University, Yokohama, Kanagawa, Japan

[§]Department of Gynecology, Yokohama City University Graduate School of Medicine, Yokohama, Kanagawa, Japan

[∥]Bioscience Division, Reagent Development Department, Tosoh Corporation, Ayase, Kanagawa, Japan

[⊥]Research Institute, Kanagawa Cancer Center, Yokohama, Kanagawa, Japan

S *Supporting Information*

ABSTRACT: Of all of the epithelial ovarian cancers (EOC), clear cell adenocarcinoma (CCA) has the worst clinical prognosis. Furthermore, the conventional EOC biomarker CA125 is more often negative in CCA than in other subtypes of EOC. This study sought to discover a new diagnostic biomarker that would allow more reliable detection of CCA. Using mass spectrometry, we compared proteins in conditioned media from cell lines derived from CCA and other types of EOC. We identified 30 extracellular or released proteins specifically present in CCA-derived cell lines. Bioinformatics analyses identified a serine protease inhibitor, tissue factor pathway inhibitor 2 (TFPI2), as a potential biomarker for CCA. Real time RT-PCR and Western blot analyses revealed that TFPI2 was exclusively expressed in CCA-derived cell lines and tissues. For clinical validation, we measured levels of TFPI2 and CA125 in a set of sera from 30 healthy women, 30 patients with endometriosis, and 50 patients with CCA, using an automated enzyme-linked immunosorbent assay systems. Serum levels of TFPI2 were significantly elevated in CCA patients, even those with normal CA125 levels. In terms of area under the receiver operating characteristic curve (AUC), TFPI2 was superior to CA125 in discriminating CCA patients from healthy women (AUC 0.97 for TFPI2 versus AUC 0.80 for CA125), or from patients with endometriosis (AUC 0.93 for TFPI2 versus 0.80 for CA125). This is the first evidence for TFPI2 as a serum biomarker of CCA. We propose that this biomarker may be useful for detection of CCA and for monitoring the transformation from endometriosis into CCA.

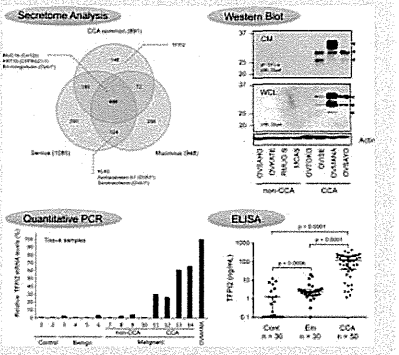

KEYWORDS: *ovarian cancer, clear cell adenocarcinoma, biomarker, diagnosis, TFPI2*

INTRODUCTION

Ovarian cancer is a leading cause of death among gynecological malignancies. Epithelial ovarian cancer (EOC), which represents the majority of ovarian cancers, is both morphologically and biologically heterogeneous.[1] Among EOC subtypes, ovarian clear cell adenocarcinoma (CCA) is a highly malignant histological type of EOC. More patients with CCA are diagnosed during stage I than patients with other types of EOC; however, they exhibit weaker responses to standard platinum-based chemotherapy, resulting in worse clinical prognoses.[2] Recurrence of CCA is higher than other types of EOC, even in early stages.[3] CCA cells exhibit relatively low proliferation activity, providing one explanation of the weak response to chemotherapy.[4,5] Therefore, earlier diagnosis and monitoring of CCA are vital.

Currently, cancer antigen 125 (CA125/MUC16) is the most frequently used clinical biomarker for EOC. However, CA125 is often negative in the early stages of EOC (only 23% positive in stage I, in contrast to more than 80% in advanced EOC).[6] Even though CA125 correlates with late-stage serous-type EOC, it is not a reliable marker for CCA: CA125 is frequently present at normal levels even at advanced stages of CCA.[7,8] Furthermore, elevation of CA125 level is also observed in benign tumors such as endometriosis,[9] which is thought to be a risk factor of CCA.[10] Therefore, the identification of a new biomarker is needed to detect of CCA efficiently.

Proteomics technology allows the high-throughput identification of thousands of proteins in complex mixtures. This technology has been applied to cancer biomarker discovery. Comprehensive proteome analyses using CCA-derived cell lines and tissues have identified several CCA-associated proteins, including annexin A4.[11,12] However, very few of the proteins identified in this manner have been shown to be serum/plasma markers potentially useful for diagnosis of CCA. To identify optimal biomarkers, it is important to consider whether the

Received: March 30, 2013
Published: June 28, 2013

ACS Publications © 2013 American Chemical Society

Table 1. Numbers of Unique Peptides Identified and Extracted Go Terms of Conventional Serum Biomarkers and 30 CCA-Specific Biomarker Candidates

			unique peptides						
			clear cell				serous	mucinous	
Uniprot accession	gene symbol	protein name	OVTOKO	OVISE	OVMANA	OVSAYO	OVSAHO, OVKATE	RMUGS, MCAS	extracted GO terms (cellular component)
known biomarker									
P02647	*APOA1*	apolipoprotein A-I	1	1	1	1	1	7	extracellular region, extracellular space, plasma membrane
P61769	*B2M*	β-2-microglobulin	2	4	3	4	4	4	extracellular region, extracellular space, plasma membrane
Q92876	*KLK6*	kallikrein-6		10		11	11	6	extracellular region
P08727	*KRT19*	keratin, type I cytoskeletal 19		10	13	16	19	3	other GO terms
Q8WXI7	*MUC16*	mucin-16	1	2	1	17	4	10	extracellular region, extracellular space, plasma membrane,
P02787	*TF*	serotransferrin	1	1			3	3	extracellular region
P02766	*TTR*	transthyretin							extracellular region
Q14508	*WFDC2*	WAP four-disulfide core domain protein 2						2	extracellular region, extracellular space
P07288	*KLK3*	prostate-specific antigen							extracellular region
CCA-specific biomarker candidates									
Q9UHI8	*ADAMTS1*	A disintegrin and metalloproteinase with thrombospondin motifs 1	2	1		3			extracellular region
Q86SJ2	*AMIGO2*	amphoterin-induced protein 2	5	2		1			plasma membrane
P18085	*ARF4*	ADP-ribosylation factor 4		1	1	2			plasma membrane
P54709	*ATP1B3*	sodium/potassium-transporting ATPase subunit β-3		1	1	1			plasma membrane
P43251	*BTD*	biotinidase	5	2		2			extracellular space, extracellular region
Q9Y5K6	*CD2AP*	CD2-associated protein		4	2	1			plasma membrane
O95832	*CLDN1*	claudin-1	1	1	1	2			plasma membrane
O60610	*DIAPH1*	protein diaphanous homologue 1		1	2	1			plasma membrane
Q6E0U4	*DMKN*	dermokine		4	3	2			extracellular space, extracellular region
Q9NZ08	*ERAP1*	endoplasmic reticulum aminopeptidase 1	7	3	5	5			extracellular region
P54652	*HSPA2*	heat shock-related 70 kDa protein 2	1	2	1	3			cell surface
P05231	*IL6*	interleukin-6	5	9	4				extracellular space, extracellular region
P78504	*JAG1*	protein jagged-1		2	1	2			extracellular region, plasma membrane
Q9UIQ6	*LNPEP*	leucyl-cystinyl aminopeptidase		1	1	1			extracellular region, plasma membrane
Q13564	*NAE1*	NEDD8-activating enzyme E1 regulatory subunit	1	1	1	2			plasma membrane
Q92597	*NDRG1*	protein NDRG1	2	2	1	1			plasma membrane
Q14112	*NID2*	nidogen-2	30	43	37	34			extracellular region
Q8IVI9	*NOSTRIN*	nostrin	1	1	1	1			plasma membrane
Q92823	*NRCAM*	neuronal cell adhesion molecule	3	3	9	13			plasma membrane
Q9NVD7	*PARVA*	α-parvin	1	1	1				plasma membrane
Q13162	*PRDX4*	peroxiredoxin-4		5	2	3			extracellular space, extracellular region
Q15907	*RAB11B*	ras-related protein Rab-11B		2	2	3			plasma membrane
P51148	*RAB5C*	ras-related protein Rab-5C		3	2	1			plasma membrane
P61006	*RAB8A*	ras-related protein Rab-5C		2	1	1			plasma membrane
Q96QD8	*SLC38A2*	sodium-coupled neutral amino acid transporter 2		1	1	1			plasma membrane
Q00796	*SORD*	sorbitol dehydrogenase		2	1	3			extracellular space
Q15833	*STXBP2*	syntaxin-binding protein 2		1	1	1			plasma membrane
P20062	*TCN2*	transcobalamin-2	7		4	11			extracellular space, extracellular region
P48307	*TFPI2*	tissue factor pathway inhibitor 2		5	8	1			extracellular region
P98155	*VLDLR*	very low-density lipoprotein receptor	5	6	3	13			extracellular space, plasma membrane

proteins of interest can actually be detected in serum/plasma samples. Furthermore, identification of biomarkers from serum or plasma using proteomics technology also has inherent limitations. Serum/plasma proteomes predominantly consist of highly abundant proteins, including albumin and immunoglobulins, which represent over 90% of the identifiable proteins within such samples. Even after depletion of the highly abundant proteins and extensive fractionation, characterization of the low-abundance proteins remains difficult.[13]

The diverse set of proteins secreted or released from cells, including proteins shed from their surface, is referred to as the "secretome". In cancer progression, multiple characteristic proteins are released from tumor cells. These proteins include growth factors and cytokines, which play important roles in cell signaling, communication, and migration. Many of these proteins enter the circulation, allowing them to be detected in patient blood samples. Thus, secretome proteins are likely to be useful as diagnostic markers of cancer.[14]

In this study, we performed secretome analysis of CCA-derived cell lines in order to discover novel clinical biomarkers that are specific to CCA, i.e., not expressed in cell lines derived from other types of EOC. In our bioinformatics analysis, we identified tissue factor pathway inhibitor 2 (TFPI2), a serine protease inhibitor, as a potential biomarker. This protein was validated as a serum marker in patients with CCA.

MATERIAL AND METHODS

Ovarian Cancer Cell Lines

CCA-derived cell lines, OVTOKO, OVISE, OVMANA, and OVSAYO, and ovarian serous adenocarcinoma-derived cell lines, OVSAHO and OVKATE were established as described previously.[15,16] Ovarian mucinous adenocarcinoma-derived cell lines, RMUG-S and MCAS were purchased from the Japanese Collection of Research Bioresources (JCRB, Osaka, Japan). All cell lines were maintained in RPMI1690 medium (Nacalai tesque, Kyoto, Japan) containing 10% fetal bovine serum (FBS, Gibco) in a humidified incubator at 37 °C under 5% CO2. The cultures were maintained for no more than 10 passages after recovery from frozen stocks.

Sample Preparation for Proteomic Analysis

For secretome analysis, the media were replaced with serum-free media supplemented with 4 nM epidermal growth factor (Invitrogen, Carlsbad, CA). After incubation for 48 h, conditioned media were collected and lyophilized. The lyophilized media were dissolved in 2 mL of 10 mM ammonium bicarbonate containing 4 M urea, and proteins were precipitated with acetone for desalting and concentration. Precipitated protein was resuspended with 10 mM ammonium bicarbonate containing 4 M urea and 0.1% RapiGest detergent (Nihon Waters, Tokyo, Japan), and used for proteomic analysis. Protein samples from serous-type cell lines (OVSAHO and OVKATE) or mucinous-type cell lines (RMUG-S and MCAS) were combined such that each pooled sample contained equal quantities of protein. The mixed samples and individual samples from CCA cell lines were used for proteomic analysis.

Proteomic Analysis

Protein (10 μg) was reduced with 10 mM DTT, and then alkylated with 25 mM iodoacetamide. The resulting alkylated protein was digested with trypsin overnight at 37 °C. Peptides were analyzed using an LC–MS/MS system consisting of a reversed-phase (RP) LC and an LTQ Orbitrap mass spectrometer (Thermo Fisher Scientific Inc., Waltham, MA, U.S.). Peptides from 3 μg of protein were analyzed in each run; this analysis was repeated three times per sample.

RPLC was performed in a 115-min acetonitrile gradient (4–40%). The RPLC effluent was interfaced with an electrospray ionization source in positive ion mode on the mass spectrometer. Protonated peptides were analyzed sequentially for MS/MS in Data-Dependent Scanning mode, consisting of a full-range scan at an m/z range of 350–1200 and subsequent product ion scans for each of the three most intense ions in the full-scan mass spectrum. Data analysis was performed using the Proteome Discoverer 1.3 software (Thermo Scientific) with Mascot ver. 2.3.02 (Matrix Science, London, U.K.). The peptide mass tolerance was set to 3 ppm and 0.5 Da for MS/MS fragmentation ions. Trypsin was set as the protease with two missed cleavage sites allowed. Cysteine carbamidomethylation and methionine oxidation were searched as a variable modification. MS/MS data were used to search for corresponding amino-acid sequences in the Swiss-Prot database (http://expasy.org/sprot). All spectra were queried against the target/decoy database to achieve a targeted false-discovery rate of 1% for all samples, using the Proteome Discoverer software.

Tissues and Sera

This study included a total of twelve tissue samples taken from four patients with CCA, four patients with other ovarian cancers, and four patients with malignant tumors, treated between 2002 and 2005. These tissue samples were taken from freshly isolated surgical resections in the operating room, rinsed thoroughly with saline, and snap-frozen in liquid nitrogen. Frozen tissues were stored at −80 °C until use. Documented informed consent was obtained from each patient, and the study was performed in accordance with the guidelines of the Ethical Committee of Yokohama City University Graduate School of Medicine. All cases were reviewed and histopathologically diagnosed by a pathologist. These tissue samples were used for *TFPI2* gene-expression analyses. In addition, commercially available total RNA samples from normal ovaries were purchased from Zyagen Laboratories (San Diego, CA, U.S.) and Ambion (Austin, TX, U.S.) and used as healthy controls in the gene-expression analyses. Numbers of unique peptides identified and extracted GO terms of conventional serum biomarkers and 30 CCA-specific biomarker candidates (Table 1). The corresponding clinicopathological data are shown in Table 2.

For the serum TFPI2 assay, a total of 110 female serum samples (collected between 1989 and 2011) were obtained from the following bioresource banks: 50 sera from patients with CCA were obtained from SLR Research Corporation (Carlsbad, CA, USA) and NOVA Biologics (Oceanside, CA, U.S.); 30 sera from patients with ovarian endometriosis were obtained from ProMedDx (Norton, MA, U.S.); and 30 sera from healthy women controls were purchased from SLR Research Corporation. These serum samples were biobank materials collected under IRB-approved protocol or as informed-consent donor samples. All samples were also stored at −80 °C until use. The corresponding clinicopathological data are shown in Table 3.

Real-Time RT-PCR

For mRNA expression analysis, total RNA was isolated from tissue samples and cell lines using the RNeasay Plus Micro Kit (Qiagen). The one step real-time RT-PCR analysis was carried out using the One-Step SYBR PrimeScript PLUS RT-PCR Kit according to the manufacturer's instructions. The analysis was performed using the Mx3000P Real-Time QPCR System

Table 2. Clinicopathological Characteristics of Tissue Samples

sample ID	source	age (years)	tissue types	clinical stages
1	Ambion	92	normal	
2	Zyagen	46	normal	
3	YCU[a]	27	simple cyst adenoma	
4	YCU[a]	47	mucinous cyst adenoma	
5	YCU[a]	56	serous cyst adenoma	
6	YCU[a]	39	mature teranoma	
7	YCU[a]	67	mucinous adenocarcinoma	3c
8	YCU[a]	31	mucinous adenocarcinoma	1a
9	YCU[a]	45	serous adenocarcinoma	3c
10	YCU[a]	54	serous adenocarcinoma	2c
11	YCU[a]	54	CCA	1a
12	YCU[a]	62	CCA	3c
13	YCU[a]	42	CCA	1c
14	YCU[a]	55	CCA	1a

[a]YCU = Yokohama City University Hospital.

Table 3. Clinicopathological Characteristics of Serum Samples

characteristics	healthy woman controls (n = 30)	endometriosis (n = 30)	CCA (n = 50)
Biobank			
SLR Research	30		30
ProMedDx		30	
NOVA Biologics			20
age (years)			
≤39	17	13	0
40 ≤ 49	8	16	9
50 ≤ 59	5	1	25
≥60	0	0	16
mean age (range)	38.3 (24–51)	39.7 (30–56)	56.8 (42–71)
classification		rAFS	FIGO
stage I		5	15
stage II		11	28
stage III		9	7
stage IV		5	0
total number	30	30	50

(Agilent Technologies, Santa Clara, CA, U.S.). *TFPI2* mRNA levels were normalized against those of *ACTB* (β-actin). Primer sequences were as follows: *TFPI2*, 5′-TGGTTAGCAGGGAGGATTGC-3′ (sense) and 5′-TCCGGATTCTACTGGCAAAG-3′ (antisense); β-actin, 5′-GATGCAGAAGGAGATCACTGC-3′ (sense) and 5′-ATACTCCTGCTTGCTGATCCAC-3′ (antisense).

Immunoprecipitation and Western Blot

Immunoprecipitation was conducted using mouse anti-TFPI2 monoclonal antibodies TF1-4 or TF1-6 (Tosoh Bioscience, Tokyo, Japan) with antimouse IgG-conjugated Dyna Magnet beads (Invitrogen). Immunoprecipitates were eluted in SDS-sample buffer and resolved by 12.5% SDS-PAGE. To detect TFPI2 protein, Western blots were carried out using the anti-TFPI2 28Aa mouse monoclonal antibody, which was raised against the *N*-terminal peptide of TFPI2 as described.[17] Antiactin antibody I-19 was purchased from Santa Cruz Biotechnology (Santa Cruz, CA). These primary antibodies were detected with the peroxidase-conjugated antimouse IgG TrueBlot antibody (eBioscience, San Diego, CA), and visualized with enhanced chemiluminescence detection.

TFPI2 and CA125 Assays

TFPI2 levels in samples were measured on an automated enzyme-linked immunosorbent assay (ELISA) system using a combination of anti-TFPI2 monoclonal antibodies, TF1-4 antibody conjugated with a magnet beads and TF1-6 antibody labeled with alkaline phosphatase. This is performed from binding reaction to fluorometric detection with an automated immunoassay analyzer system (Tosoh) as described previously.[18] The calibration standard for TFPI2 was prepared from the conditioned medium of HEK293-T cells transfected with the recombinant TFPI2 expression vector; the standard was spiked into FBS for the ELISA. Serum level of CA125 was assessed with a commercially available extracorporeal diagnostic kit, E test TOSOH II CA125 (Tosoh) according to the manufacture's instructions. Both automated ELISA were performed using the AIA-1800 analyzer machine (Tosoh). Results of each assay were confirmed to meet the following criteria: coefficient of variation (CV) less than 10%; measurement within the linear standard range; and R^2 of the standard curve regression line at least 0.95.

Statistical Analysis

ELISA data were plotted as a scatter plot and a receiver operating characteristic (ROC) curves. The statistical significance of the difference between two groups was determined using the Wilcoxon test. All data were processed using GraphPad PRISM software (version 5.0). Data are expressed as means ± standard deviations.

RESULTS

Secretome Analysis

The workflow for secretome analysis is illustrated in Figure 1. Four CCA cell lines and four cell lines derived from other types of EOC were cultured in serum-free media; 50–600 μg of protein were obtained from 20-mL samples of conditioned media. These protein samples were analyzed by LC–MS/MS as described above in Materials and Methods. Protein samples from CCA cell lines were individually examined to find proteins common to these cell lines. In the LC–MS/MS analyses, 3029–4514 unique peptides were identified from CCA cell lines, mapping to a total of 896–1231 unique proteins. In addition, analyses of serous- and mucinous-type cell lines were also performed after pooling according to histological type, to reveal proteins which should not be selected as CCA-marker candidates. In the pooled sample of the serous-type cell lines, OVSAHO and OVKATE, 3491–3702 unique peptides were identified, mapping to total of 1085 unique proteins; in the pooled sample of the mucinous-type cell lines, RMUG-S and MCAS, 3132–3197 unique peptides were identified, mapping to a total of 948 unique proteins. These data were summarized in Supplementary Table S1 of the Supporting Information, SI, and the raw information (the peptide sequences, scores, the practical mass differences, etc.) was listed in Supplementary Table S2 of the SI.

Selection of Potential CCA Marker Candidate

To choose potential CCA marker candidates from among these proteins, we searched for proteins satisfying the following criteria.

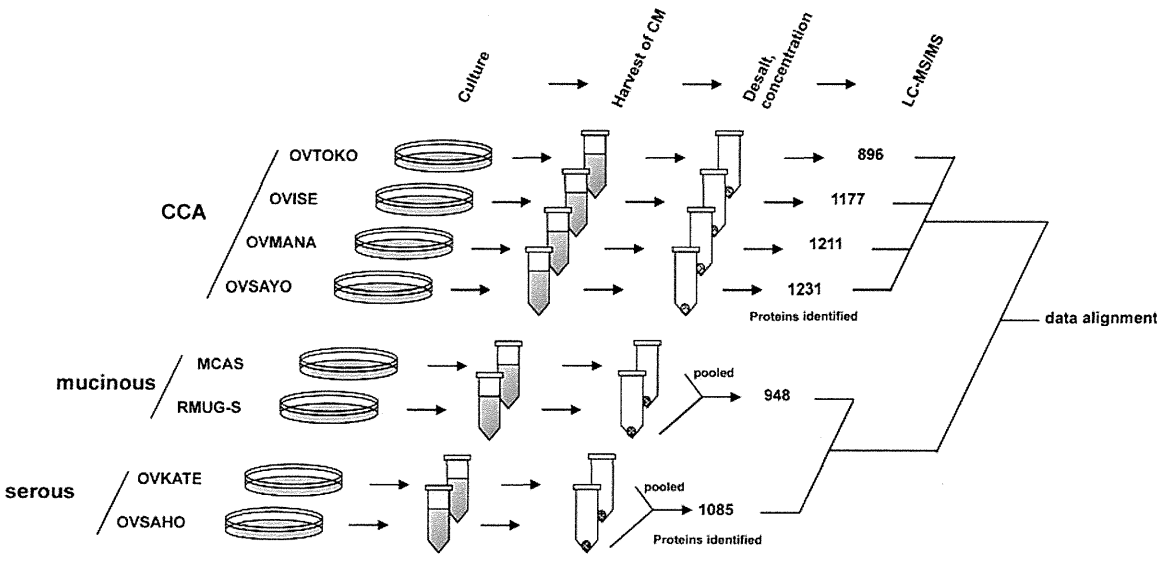

Figure 1. Secretome-based differential analysis of ovarian cancer cell lines. Experimental overview. Protein samples from CCA cell lines were individually examined, and those from serous- and mucinous-type EOC cell lines were analyzed after pooling according to each histological subtype. Total numbers of proteins identified from each sample were indicated.

First, we focused on proteins common to CCA cell lines, based on alignment of the LC–MS/MS analysis data. Of a total of 1864 proteins identified in CCA cell lines, 537 proteins were present in all four cell lines, and 354 more proteins were present in three cell lines (Figure 2A). This combined set of 891 proteins was chosen as the starting point.

Next, these 891 proteins were compared with proteins identified in cell lines derived from serous-type and mucinous-type EOC (Figure 2B). This comparative analysis revealed that 148 proteins were restricted to CCA-derived cell lines. Several known EOC markers, including Mucin 16 (MUC16, a core protein of CA125) and cytokeratin 19 (KRT19, a core protein of CYFRA19-9),[19] were identified in all EOC cell lines. In addition, β_2-microglobulin (B2M), apolipoprotein A1 (APOA1), and transferrin (TF), which are biomarkers used in FDA-cleared OVA1 test,[20] and kallilrein-6 (KLK6),[21] were also detected in samples from serous- and mucinous-type cell lines. The restricted set of 148 proteins specific to CCA cell lines was expected to contain new biomarkers that might replace conventionally used general EOC markers.

From the list of 148 CCA-restricted proteins, we searched for those classified as extracellular proteins or membrane proteins, because these proteins or their fragments are more likely to enter the circulation and to be detectable in sera. For this purpose, we queried the 148 CCA-restricted proteins against the RCAI RefDIC database (http://refdic.rcai.riken.jp/). From this search, we identified 30 proteins classified by the Gene Ontology (GO) terms "extracellular space", "extracellular region", "cell surface", and "plasma membrane"; several known biomarkers are also classified by such GO terms. Numbers of identified peptides and GO terms of known biomarkers and 30 CCA-specific biomarker candidates were summarized in Table 1.

We further investigated the gene expression profiles of 30 proteins using the RefDIC database to identify proteins that are neither abundantly nor widely expressed in other tissues. Because tumor secretome proteins would be present at trace levels early in cancer progression, the most useful biomarkers would be those for which the baseline in healthy individuals is as low as possible. In fact, gene expression patterns of several known biomarkers such as MUC16 (CA125), WFDC2 (HE4), or KLK3 (prostate cancer antigen, PSA) exhibit high tissue-specificity in the RefDIC database (Supplementary Figure S1 of the SI). Of the 30 proteins, tissue factor pathway inhibitor 2 (TFPI2), which was identified in the OVISE, OVMANA, and OVSAYO cell lines, exhibited tissue-specific expression in a pattern similar to those of known biomarkers (Supplementary Figure S1 of the SI). The Human Protein Atlas database (version 9.0, http://www.proteinatlas.org/) describes expression of TFPI2 as negative in most tissues but high in placenta (Supplementary Figure S2 of the SI). In addition, a previous DNA microarray-based study that compared several subtypes of EOC reported *TFPI2* as a CCA-specific gene.[22] Thus, we focused our attention on TFPI2 as a potential biomarker for CCA.

CCA-Specific Expression of TFPI2 Gene

To verify the expression of *TFPI2* in CCA, we performed real-time RT-PCR analysis on the 8 EOC cell lines. This analysis revealed that the *TFPI2* transcript was highly expressed in every CCA-derived cell line except for OVTOKO (Figure 3A). This result was consistent with the data from the aforementioned secretome analysis. Moreover, we also performed gene-expression analysis on 14 ovary tissue samples. *TFPI2* mRNA was also highly expressed in ovarian tissues from CCA patients, whereas it was barely detectable in patients with other EOC subtypes, benign tumors, or normal ovary tissue (Figure 3B). These data indicate that *TFPI2* expression is specific to CCA.

TFPI2 Secreted in Conditioned Media

To detect TFPI2 secreted in conditioned media from CCA cell lines, we performed immunoprecipitations using the anti-TFPI2 monoclonal antibodies TF1-4 and TF1-6, which were used as the capture antibody and detection antibody, respectively, in the automated ELISA system for TFPI2 detection. Immunoprecipitates brought down with TF1-4 or TF1-6 antibody and cell lysates were resolved on SDS-PAGE, and Western-blot analysis was carried out using a monoclonal antibody (28Aa) specific to the *N*-terminal 14 amino acid residues of TFPI2. As shown in Figure 4A,B, three TFPI2 protein isoforms, thought to represent different glycated forms (33-kDa, 32-kDa, 27-kDa isoforms),[23]

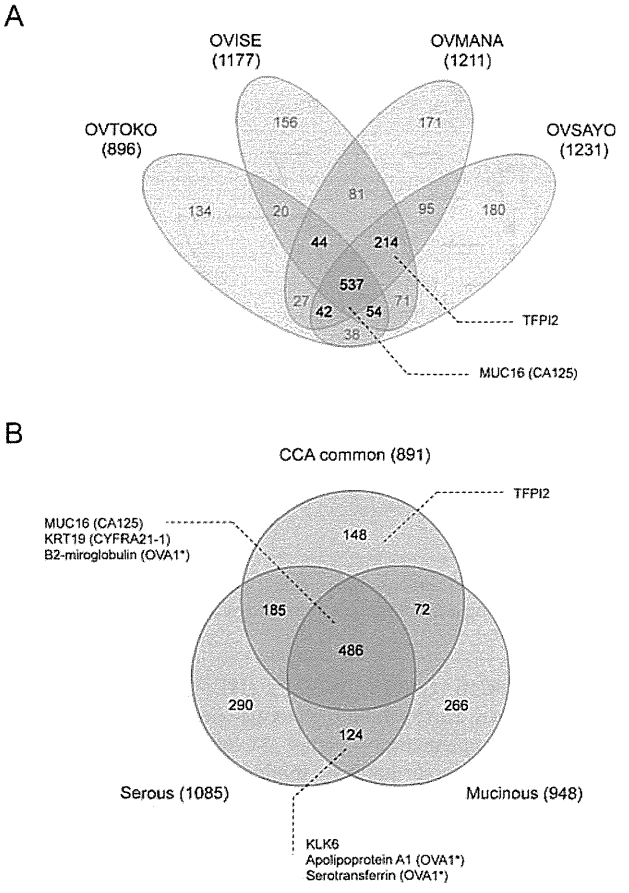

Figure 2. Overlaps of proteins identified between each sample. Venn diagrams show overlap between four CCA cell lines (A), and between the 891 proteins common to CCA cell lines and the set of proteins identified in serous- and mucinous-type EOC cell lines (B). This illustration indicates the categories that include known ovarian cancer markers and TFPI2 were identified. Asterisks indicate the biomarkers used in the OVA1 test.

were detected in conditioned media and whole cell lysates from three CCA cell lines (OVISE, OVMANA, and OVSAYO). Moreover, automated ELISA also clearly detected TFPI2 in conditioned media from these CCA cell lines (Figure 4C). The TFPI2 signals in cell lines markedly decreased upon introduction of TFPI2 siRNAs (data not shown), suggesting that the ELISA system was accurately detecting TFPI2. These results were consistent with the data from the secretome analysis and real-time RT-PCR analysis.

Serum Levels of TFPI2 in CCA Patients

Because TFPI2 was specifically expressed in CCA-derived cell lines and tissues, and could be detected in conditioned media from these cell lines, we speculated that TFPI2 would be detectable in serum samples from CCA patients. To examine this possibility, we determined TFPI2 levels by automated ELISA in serum samples from patients with CCA (n = 50), ovarian endometriosis (n = 30), and healthy women (n = 30), and compared TFPI2 levels to those of CA125 (Figure 5A and B). In the test set, serum CA125 levels were significantly higher in CCA patients (median [25th–75th percentiles], 219.5 [823.1–735.8] U/mL) than healthy women (17.0 [12.6–22.4] U/mL) or endometriosis patients (15.5 [7.2–24.0] U/mL). The levels of serum TFPI2 were also significantly higher in CCA patients (107.5 [35.2–183.0] ng/mL) compared to healthy women (<0.1 (below detection limit) [<0.1–1.2] ng/mL) or endometriosis samples (2.2 [1.5–3.0] ng/mL). TFPI2 levels in CCA patients were not statistically correlated with age or tumor stage (Figure 5C and D). These findings support the use of TFPI2 as a novel biomarker for CCA detection.

Efficacy of TFPI2 and CA125 for CCA Diagnosis

To further evaluate the diagnostic efficacy of TFPI2, we conducted a receiver operating characteristic (ROC) curve analysis. The area under the ROC curves (AUC) for TFPI2 and CA125 were compared between CCA patients and either healthy controls or endometriosis patients. The analyses revealed that TFPI2 was superior to CA125 in discriminating CCA patients from healthy controls (AUC = 0.97 [95% CI, 0.94–1.00] versus AUC = 0.80 [95% CI, 0.70–0.90]; Figure 6A) and endometriosis patients (AUC = 0.93 [95% CI, 0.88–1.00] versus AUC = 0.80

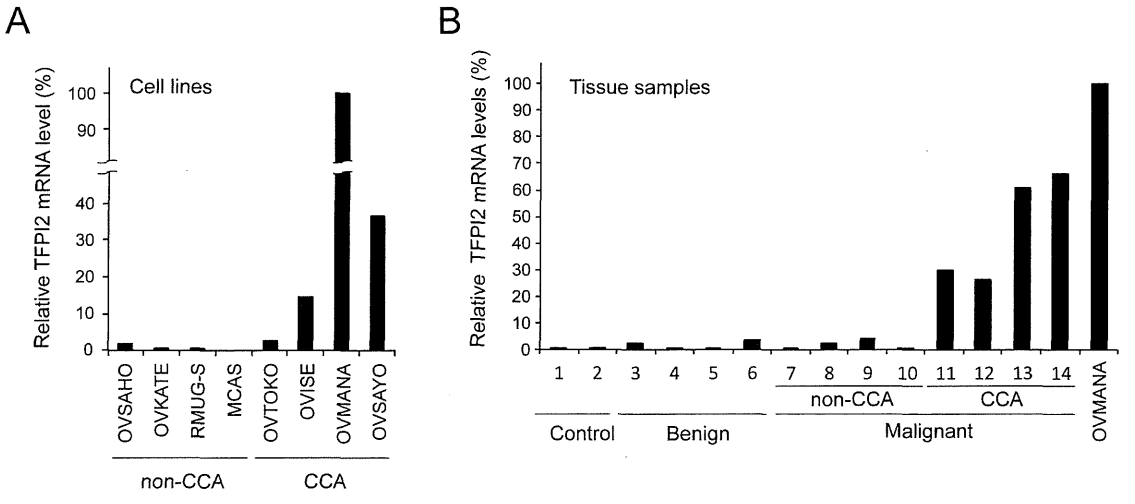

Figure 3. CCA-specific expression of TFPI2 gene. *TFPI2* mRNA levels in ovarian cancer cell lines (A) and various ovarian tissue samples (B) were evaluated by real-time PCR. Data were normalized against β-actin mRNA levels. The corresponding clinicopathological data from these tissue samples are shown in Table 2.

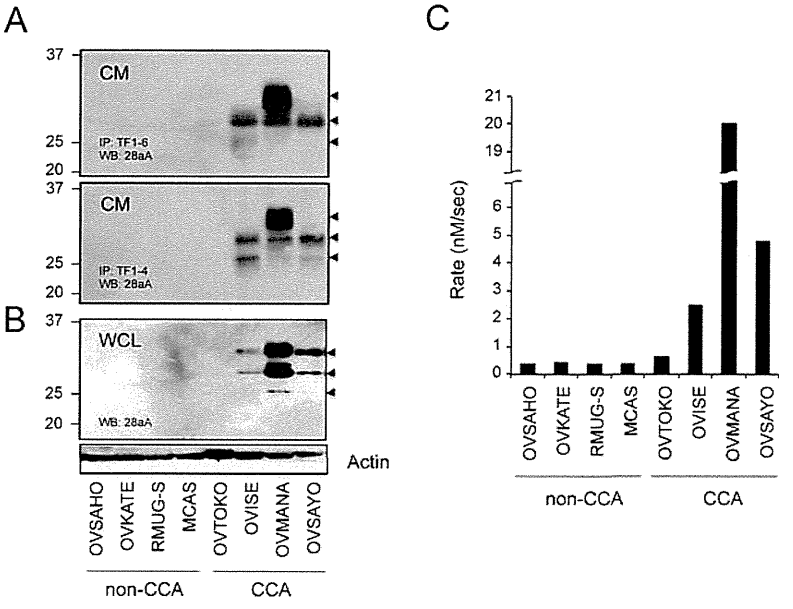

Figure 4. Detection of secreted TFPI2 in condition media. TFPI2 in conditioned media (CM, A) and whole-cell lysate (WCL, B) were detected by Western blot. Aliquots of conditioned media (0.5 mL) were subjected to immunoprecipitation with either TF1-6 or TF1-4 monoclonal antibodies. Precipitates or whole-cell lysates were resolved by denaturing SDS-PAGE, and TFPI2 was detected by Western blot using the 28aA anti-TFPI2 monoclonal antibody. (C) TFPI2 in conditioned media was determined using an automated ELISA system.

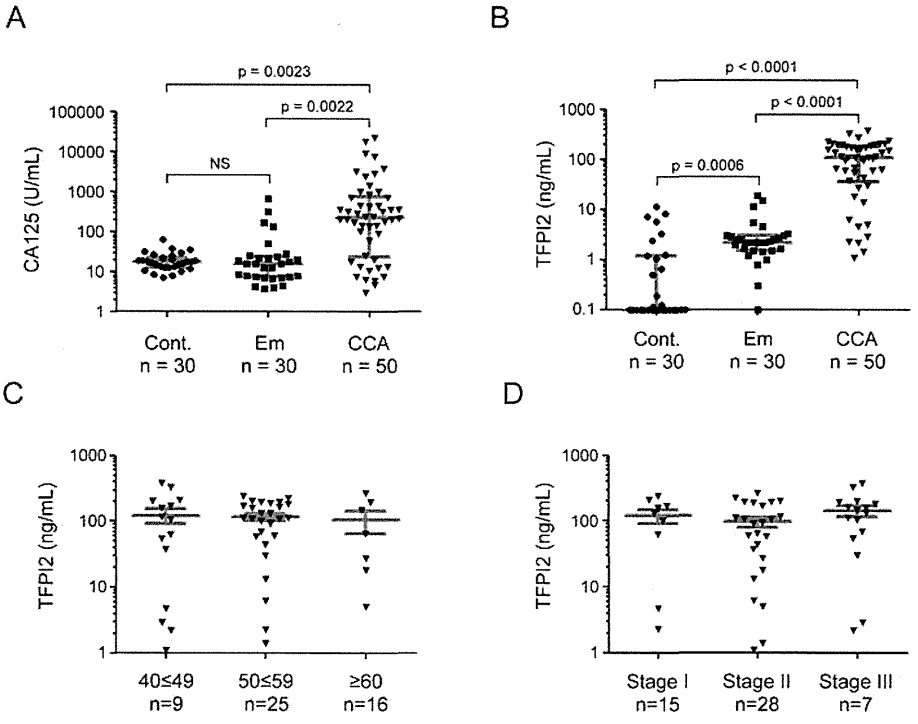

Figure 5. Serum levels of CA125 and TFPI2 in CCA patients. The serum levels of CA125 (A) and TFPI2 (B) were measured in 50 CCA patients, 30 endometriosis patients (Em), and 30 healthy controls (Cont.). The corresponding clinicopathological data from these serum samples are summarized in Table 3. (C, D) Serum TFPI2 levels in CCA patients, grouped by age (C) and tumor stage (D). Middle horizontal line indicates the median; upper and lower lines indicate the 25th and 75th percentiles of the data range, respectively. TFPI2 levels under detection limit (0.1 ng/mL) were represented as 0.1 ng/mL.

[95% CI, 0.71–0.90]; Figure 6B). When a cutoff value of 12.3 ng/mL was chosen for TFPI2, the sensitivity and specificity of discrimination between CCA patients and healthy controls were 84% and 100%, respectively. For discrimination between CCA patients and endometriosis, sensitivity and specificity were 84% and 93%, respectively.

In general, patients with CCA have lower CA125 levels more frequently than patients with other EOC subtypes.[7,8] Of the 50

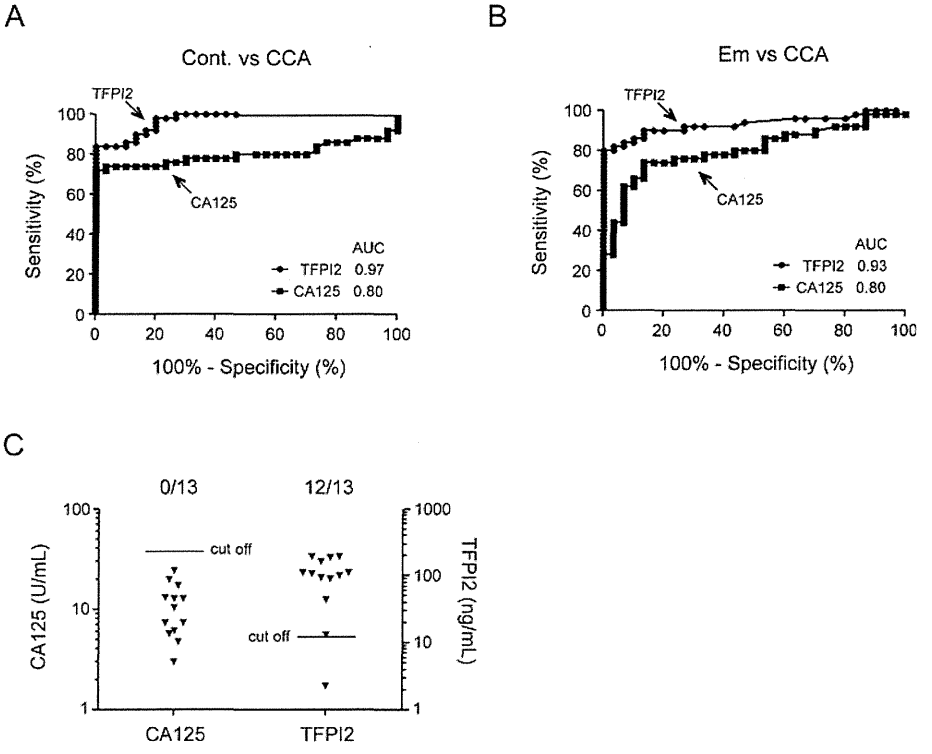

Figure 6. Efficacy of TFPI2 for CCA detection. (A, B) ROC curve analyses of the ability of CA125 and TFPI2 to discriminate between healthy controls and CCA patients (A), and between endometriosis and CCA patients (B). (C) TFPI2 levels in sera from 13 patients with normal CA125 levels (<35 U/mL). Cutoff values of CA125 (35 U/mL) and TFPI2 (12.3 ng/mL) are indicated with lines.

CCA patients in the test set, 13 patients had CA125 levels below 35 U/mL, the currently applied cutoff value for ovarian cancer screening. Applying a cutoff value 12.3 ng/mL for TFPI2, we found that 12 of 13 CCA patients with normal CA125 levels (<35 U/mL) were positive for TFPI2 (Figure 6C). Collectively, these results indicate that the diagnostic accuracy of TFPI2 was higher than that of CA125.

DISCUSSION

EOC is a heterogeneous disease, and each histological subtype exhibits distinct clinical characteristics, morphology, and biological behavior.[1] Among EOC subtypes, CCA exhibits a weaker response to standard platinum-based chemotherapy, and therefore has a markedly worse clinical prognosis. Furthermore, CCA cannot be reliably detected using CA125; whereas over 90% of patients with endometrioid-type and serous-type EOC show exhibit high levels of serum CA125, only 61% of patients with CCA are positive for this biomarker.[7] Therefore, identification of new biomarker is necessary in order to improve the detection efficiency of CCA and overcome the diagnostic limitations of CA125.

In the present study, we performed secretome analysis of cultured CCA-derived cell lines to identify optimal biomarker for CCA. We first examined proteins common to CCA cell lines by individual analysis of four cell lines (Figure 2A). Then, we focused our attention on not only 537 proteins that were overlapped in all four CCA cell lines, but also 354 proteins that were identified only in three CCA cell lines, because we assumed that a cell line that decreased or lost gene expression of a useful marker candidate might be present. From the combined set of 891 proteins, we next eliminated proteins identified in cell lines derived from other types of EOC (Figure 2B), and extracted "extracellular proteins" and "membrane proteins" using database information (Table 1). This analysis revealed that 30 proteins were specifically detected in conditioned media of CCA cell lines. Of these 30 proteins, only TFPI2 expression exhibited markedly higher tissue specificity in both mRNA (RefDIC) and protein (Human Protein Atlas) databases. In addition, a previous DNA microarray-based study suggests TFPI2 expression in ovarian tissues from CCA patients,[22] but there is no report on TFPI2 expression in blood samples from cancer patients. Thus, we focused our attention on TFPI2 as a new biomarker candidate for CCA diagnosis.

In our validation study, *TFPI2* mRNA was exclusively expressed in CCA-derived cell lines and tissues (Figure 3), and secreted TFPI2 was also clearly detected in CCA cell lines, with the exception of the OVTOKO cell line, in line with secretome analysis data (Figure 4). TFPI2 assay using automated ELISA revealed that serum TFPI2 levels discriminated CCA patients not only from healthy women, but also from patients with endometriosis (Figure 5), with a higher diagnostic accuracy than that of CA125 (Figure 6A,B). This is the first report that serum TFPI2 might be useful for CCA diagnosis. Although some secretome analyses aimed at discovery of potential serum biomarkers for ovarian cancer have already been reported,[14] very few of those reports discussed diagnostic accuracy for CCA. Importantly, we found that TFPI2 exhibited a higher rate (12/13) in CCA patients with normal levels of CA125 (Figure 6C). Thus, use of TFPI2 as a biomarker might allow identification of CCA patients who are not diagnosed on the basis of CA125.

CCA is thought to arise, at least in part, from endometriosis; 50% of CCA and 40% of endometrioid-type ovarian cancers are associated with endometriosis.[24] Furthermore, endometriosis increases the risk of ovarian cancer, especially CCA.[10] Therefore,

it is very important to carefully monitor the transformation from endometriosis into CCA. However, CA125 levels do not permit reliable monitoring, because this biomarker has low sensitivity in identifying patients with CCA (as well as early stage EOC).[6] Furthermore, CA125 has a high false-positive rate in patients with endometriosis.[25] In contrast, serum TFPI2 levels could discriminate between patients with CCA and endometriosis with higher sensitivity (84%) and specificity (93%) than CA125. Thus, we believe that the use of TFPI2, alone or in combination with CA125, would improve the accuracy of CCA diagnosis.

TFPI2, also known as placental protein 5 (PP5),[26,27] is abundantly produced in placenta and can be detected in the serum of pregnant women.[28] Although the function of TFPI2 during pregnancy is not fully understood, serum TFPI2 level rises significantly during pregnancy.[29,30] In addition, TFPI2 level in maternal serum changes in cases of preeclampsia or intrauterine growth restriction.[17] Therefore, the TFPI2 level in pregnant women must be interpreted carefully. In this regard, TFPI2 is similar to CA125, the level of which is also influenced significantly by pregnancy.[29]

Although the physiological role of TFPI2 has yet to be firmly established, it has been reported that TFPI2 plays a role as a mitogen for vascular smooth muscle cells and retinal pigment epithelial cells.[30,31] In the context of cancer biology, study of TFPI2 has focused on its protease inhibitor activity. TFPI2 contains three tandemly repeated Kunitz-type proteinase inhibitory domains.[32] Due to its ability to inhibit a wide range of serine proteases, including plasmin, trypsin, or chymotrypsin, it may play a critical role in the regulation of extracellular matrix (ECM) remodeling.[27,33−35] By broadly inhibiting proteases, TFPI2 may protect the ECM from degradation, thereby counteracting tumor invasion and metastasis. Consistently, many studies observed that overexpression of TFPI2 significantly suppresses cellular invasion or growth in several human cancer types, including lung, prostate, and pancreas.[36−40] TFPI2 has also been shown to induce apoptosis and inhibit angiogenesis.[41,42] Furthermore, TFPI2 expression is decreased or diminished upon aberrant methylation of the *TFPI2* promoter in various human cancers.[40,43−46] Thus, it is reasonable to consider TFPI2 as a potential tumor suppressor. In this study, by contrast, we demonstrated that the *TFPI2* gene was exclusively expressed in CCA cell lines and tissues (Figure 3). This finding is in agreement with a previous report, based on a DNA-microarray study, that the *TFPI2* gene is upregulated in CCA tissues relative to other histological subtype of EOC.[22] More patients with CCA are diagnosed during stage I than patients with other types of EOC.[2] Taken together, these observations suggest that TFPI2 helps to maintain CCA in the early stage by regulating the invasion and growth activity of the tumor cells.

In conclusion, we have identified the serine protease inhibitor TFPI2 as potential biomarker for CCA detection. An analysis of the area under the ROC curve showed that TFPI2 was superior to CA125 in discriminating CCA patients from healthy controls or patients with endometriosis. Although this finding awaits further validation in sera of patients with other EOC subtypes and tumors from other tissues, TFPI2 nonetheless holds great promise as a diagnostic biomarker for CCA.

■ ASSOCIATED CONTENT

Supporting Information

Supplementary Table S1: Numbers of proteins identified in each sample. Supplementary Table S2: The raw information of protein identification. Supplementary Figure S1: Gene-expression profiles of conventional biomarkers and 30 CCA-specific biomarker candidates in the RefDIC database. Supplementary Figure S2: Expression profile of TFPI2 in the Human Protein Atlas using CAB10142 antibody. This material is available free of charge via the Internet at http://pubs.acs.org.

■ AUTHOR INFORMATION

Corresponding Author

*Tel: +81-45-787-2322; fax: +81-45-787-2787; e-mail: arakawa@yokohama-cu.ac.jp (N.A.), hirano@yokohama-cu.ac.jp (H.H).

Notes

The authors declare no competing financial interest.

■ ACKNOWLEDGMENTS

This work was supported in part by the Special Coordination Funds for Promoting Science and Technology "Creation of Innovation Centers for Advanced Interdisciplinary Research Areas" (to H.H.), and in part by Grants-in-Aid, Research on Biological Markers for New Drug Development H20-0005 (to H.H.), and Grant-in-Aid for young Scientists (B) 22790530 from The Ministry of Education, Culture, Sports, Science and Technology (to N.A.) of Japan.

■ REFERENCES

(1) Cho, K. R.; Shih, Ie, M. Ovarian Cancer. *Ann. Rev. Pathol.* **2009**, *4*, 287−313.

(2) Itamochi, H.; Kigawa, J.; Terakawa, N. Mechanisms of Chemoresistance and Poor Prognosis in Ovarian Clear Cell Carcinoma. *Cancer Sci.* **2008**, *99* (4), 653−658.

(3) Sugiyama, T.; Kamura, T.; Kigawa, J.; Terakawa, N.; Kikuchi, Y.; Kita, T.; Suzuki, M.; Sato, I.; Taguchi, K. Clinical Characteristics of Clear Cell Carcinoma of the Ovary: A Distinct Histologic Type with Poor Prognosis and Resistance to Platinum-Based Chemotherapy. *Cancer* **2000**, *88* (11), 2584−2589.

(4) Itamochi, H.; Kigawa, J.; Akeshima, R.; Sato, S.; Kamazawa, S.; Takahashi, M.; Kanamori, Y.; Suzuki, M.; Ohwada, M.; Terakawa, N. Mechanisms of Cisplatin Resistance in Clear Cell Carcinoma of the Ovary. *Oncology* **2002**, *62* (4), 349−353.

(5) Itamochi, H.; Kigawa, J.; Sugiyama, T.; Kikuchi, Y.; Suzuki, M.; Terakawa, N. Low Proliferation Activity May Be Associated with Chemoresistance in Clear Cell Carcinoma of the Ovary. *Obstet. Gynecol.* **2002**, *100* (2), 281−287.

(6) Suh, K. S.; Park, S. W.; Castro, A.; Patel, H.; Blake, P.; Liang, M.; Goy, A. Ovarian Cancer Biomarkers for Molecular Biosensors and Translational Medicine. *Exp. Rev. Mol. Diagn.* **2010**, *10* (8), 1069−1083.

(7) Kudoh, K.; Kikuchi, Y.; Kita, T.; Tode, T.; Takano, M.; Hirata, J.; Mano, Y.; Yamamoto, K.; Nagata, I. Preoperative Determination of Several Serum Tumor Markers in Patients with Primary Epithelial Ovarian Carcinoma. *Gynecol. Obstet. Invest.* **1999**, *47* (1), 52−57.

(8) Pectasides, D.; Fountzilas, G.; Aravantinos, G.; Kalofonos, C.; Efstathiou, H.; Farmakis, D.; Skarlos, D.; Pavlidis, N.; Economopoulos, T.; Dimopoulos, M. A. Advanced Stage Clear-Cell Epithelial Ovarian Cancer: The Hellenic Cooperative Oncology Group experience. *Gynecol. Oncol.* **2006**, *102* (2), 285−291.

(9) Meyer, T.; Rustin, G. J. Role of Tumour Markers in Monitoring Epithelial Ovarian Cancer. *Br. J. Cancer* **2000**, *82* (9), 1535−1538.

(10) Nagle, C. M.; Olsen, C. M.; Webb, P. M.; Jordan, S. J.; Whiteman, D. C.; Green, A. C. Endometrioid and Clear Cell Ovarian Cancers: A Comparative Analysis of Risk Factors. *Eur. J. Cancer* **2008**, *44* (16), 2477−2484.

(11) Morita, A.; Miyagi, E.; Yasumitsu, H.; Kawasaki, H.; Hirano, H.; Hirahara, F. Proteomic Search for Potential Diagnostic Markers and

Therapeutic Targets for Ovarian Clear Cell Adenocarcinoma. *Proteomics* **2006**, *6* (21), 5880–5890.
(12) Kim, A.; Enomoto, T.; Serada, S.; Ueda, Y.; Takahashi, T.; Ripley, B.; Miyatake, T.; Fujita, M.; Lee, C. M.; Morimoto, K.; Fujimoto, M.; Kimura, T.; Naka, T. Enhanced Expression of Annexin A4 in Clear Cell Carcinoma of the Ovary and Its Association with Chemoresistance to Carboplatin. *Int. J. Cancer* **2009**, *125* (10), 2316–2322.
(13) Anderson, N. L.; Anderson, N. G.; Haines, L. R.; Hardie, D. B.; Olafson, R. W.; Pearson, T. W. Mass Spectrometric Quantitation of Peptides and Proteins Using Stable Isotope Standards and Capture by Anti-Peptide Antibodies (SISCAPA). *J. Proteome Res.* **2004**, *3* (2), 235–244.
(14) Makridakis, M.; Vlahou, A. Secretome Proteomics for Discovery of Cancer Biomarkers. *J. Proteomics* **2010**, *73* (12), 2291–2305.
(15) Gorai, I.; Nakazawa, T.; Miyagi, E.; Hirahara, F.; Nagashima, Y.; Minaguchi, H. Establishment and Characterization of Two Human Ovarian Clear Cell Adenocarcinoma Lines from Metastatic Lesions with Different Properties. *Gynecol. Oncol.* **1995**, *57* (1), 33–46.
(16) Yanagibashi, T.; Gorai, I.; Nakazawa, T.; Miyagi, E.; Hirahara, F.; Kitamura, H.; Minaguchi, H. Complexity of Expression of the Intermediate Filaments of Six New Human Ovarian Carcinoma Cell Lines: New Expression of Cytokeratin 20. *Br. J. Cancer* **1997**, *76* (7), 829–835.
(17) Ogawa, M.; Yanoma, S.; Nagashima, Y.; Okamoto, N.; Ishikawa, H.; Haruki, A.; Miyagi, E.; Takahashi, T.; Hirahara, F.; Miyagi, Y. Paradoxical Discrepancy between the Serum Level and the Placental Intensity of PP5/TFPI-2 in Preeclampsia and/or Intrauterine Growth Restriction: Possible Interaction and Correlation with Glypican-3 Hold the Key. *Placenta* **2007**, *28* (2–3), 224–232.
(18) Nakamura, K.; Igarashi, K.; Ide, K.; Ohkawa, R.; Okubo, S.; Yokota, H.; Masuda, A.; Oshima, N.; Takeuchi, T.; Nangaku, M.; Okudaira, S.; Arai, H.; Ikeda, H.; Aoki, J.; Yatomi, Y. Validation of an Autotaxin Enzyme Immunoassay in Human Serum Samples and Its Application to Hypoalbuminemia Differentiation. *Clin. Chim. Acta; Int. J. Clin. Chem.* **2008**, *388* (1–2), 51–58.
(19) Gadducci, A.; Ferdeghini, M.; Cosio, S.; Fanucchi, A.; Cristofani, R.; Genazzani, A. R. The Clinical Relevance of Serum CYFRA 21–1 Assay in Patients with Ovarian Cancer. *Int. J. Gynecol. Cancer: Off. J. Int. Gynecol. Cancer Soc.* **2001**, *11* (4), 277–282.
(20) Fung, E. T. A Recipe for Proteomics Diagnostic Test Development: The OVA1 Test, From Biomarker Discovery to FDA Clearance. *Clin. Chem.* **2010**, *56* (2), 327–329.
(21) Luo, L. Y.; Soosaipillai, A.; Grass, L.; Diamandis, E. P. Characterization of Human Kallikreins 6 and 10 in Ascites Fluid from Ovarian Cancer Patients. *Tumour Biol.: J. Int. Soc. Oncodev. Biol. Med.* **2006**, *27* (5), 227–234.
(22) Zorn, K. K.; Bonome, T.; Gangi, L.; Chandramouli, G. V.; Awtrey, C. S.; Gardner, G. J.; Barrett, J. C.; Boyd, J.; Birrer, M. J. Gene Expression Profiles of Serous, Endometrioid, And Clear Cell Subtypes of Ovarian and Endometrial Cancer. *Clin. Cancer Res.: Off. J. Am. Assoc. Cancer Res.* **2005**, *11* (18), 6422–6430.
(23) Rao, C. N.; Reddy, P.; Liu, Y.; O'Toole, E.; Reeder, D.; Foster, D. C.; Kisiel, W.; Woodley, D. T. Extracellular Matrix-Associated Serine Protease Inhibitors (Mr 33,000, 31,000, and 27,000) are Single-Gene Products with Differential Glycosylation: cDNA Cloning of the 33-kDa Inhibitor Reveals Its Identity to Tissue Factor Pathway Inhibitor-2. *Arch. Biochem. Biophys.* **1996**, *335* (1), 82–92.
(24) Sato, N.; Tsunoda, H.; Nishida, M.; Morishita, Y.; Takimoto, Y.; Kubo, T.; Noguchi, M. Loss of Heterozygosity on 10q23.3 and Mutation of the Tumor Suppressor Gene PTEN in Benign Endometrial Cyst of the Ovary: Possible Sequence Progression from Benign Endometrial Cyst to Endometrioid Carcinoma and Clear Cell Carcinoma of the Ovary. *Cancer Res.* **2000**, *60* (24), 7052–7056.
(25) Markman, M. CA-125: an Evolving Role in the Management of Ovarian Cancer. *J. Clin. Oncol.: Off. J. Am. Soc. Clin. Oncol.* **1996**, *14* (5), 1411–1412.
(26) Kisiel, W.; Sprecher, C. A.; Foster, D. C. Evidence That a Second Human Tissue Factor Pathway Inhibitor (TFPI-2) and Human Placental Protein 5 Are Equivalent. *Blood* **1994**, *84* (12), 4384–4385.
(27) Miyagi, Y.; Koshikawa, N.; Yasumitsu, H.; Miyagi, E.; Hirahara, F.; Aoki, I.; Misugi, K.; Umeda, M.; Miyazaki, K. cDNA Cloning and mRNA Expression of a Serine Proteinase Inhibitor Secreted by Cancer Cells: Identification As Placental Protein 5 and Tissue Factor Pathway Inhibitor-2. *J. Biochem.* **1994**, *116* (5), 939–942.
(28) Bohn, H.; Winckler, W. [Isolation and characterization of the placental protein pp5 (author's transl)]. *Arch. Gynakol.* **1977**, *223* (3), 179–186.
(29) Sarandakou, A.; Protonotariou, E.; Rizos, D. Tumor Markers in Biological Fluids Associated with Pregnancy. *Crit. Rev. Clin. Lab. Sci.* **2007**, *44* (2), 151–178.
(30) Shinoda, E.; Yui, Y.; Hattori, R.; Tanaka, M.; Inoue, R.; Aoyama, T.; Takimoto, Y.; Mitsui, Y.; Miyahara, K.; Shizuta, Y.; Sasayama, S. Tissue Factor Pathway Inhibitor-2 Is a Novel Mitogen for Vascular Smooth Muscle Cells. *J. Biol. Chem.* **1999**, *274* (9), 5379–5384.
(31) Tanaka, Y.; Utsumi, J.; Matsui, M.; Sudo, T.; Nakamura, N.; Mutoh, M.; Kajita, A.; Sone, S.; Kigasawa, K.; Shibuya, M.; Reddy, V. N.; Zhang, Q.; Iwata, T. Purification, Molecular Cloning, And Expression of a Novel Growth-Promoting Factor for Retinal Pigment Epithelial Cells, REF-1/TFPI-2. *Invest. Ophthalmol. Visual Sci.* **2004**, *45* (1), 245–252.
(32) Bajaj, M. S.; Birktoft, J. J.; Steer, S. A.; Bajaj, S. P. Structure and Biology of Tissue Factor Pathway Inhibitor. *Thromb. Haemost.* **2001**, *86* (4), 959–972.
(33) Sprecher, C. A.; Kisiel, W.; Mathewes, S.; Foster, D. C. Molecular Cloning, Expression, And Partial Characterization of a Second Human Tissue-Factor-Pathway Inhibitor. *Proc. Natl. Acad. Sci. U.S.A.* **1994**, *91* (8), 3353–3357.
(34) Rao, C. N.; Liu, Y. Y.; Peavey, C. L.; Woodley, D. T. Novel Extracellular Matrix-Associated Serine Proteinase Inhibitors from Human Skin Fibroblasts. *Arch. Biochem. Biophys.* **1995**, *317* (1), 311–314.
(35) Petersen, L. C.; Sprecher, C. A.; Foster, D. C.; Blumberg, H.; Hamamoto, T.; Kisiel, W. Inhibitory Properties of a Novel Human Kunitz-Type Protease Inhibitor Homologous to Tissue Factor Pathway Inhibitor. *Biochemistry* **1996**, *35* (1), 266–272.
(36) Lakka, S. S.; Konduri, S. D.; Mohanam, S.; Nicolson, G. L.; Rao, J. S. In Vitro Modulation of Human Lung Cancer Cell Line Invasiveness by Antisense cDNA of Tissue Factor Pathway Inhibitor-2. *Clin. Exp. Metastasis* **2000**, *18* (3), 239–244.
(37) Konduri, S. D.; Tasiou, A.; Chandrasekar, N.; Rao, J. S. Overexpression of Tissue Factor Pathway Inhibitor-2 (TFPI-2), Decreases the Invasiveness of Prostate Cancer Cells in Vitro. *Int. J. Oncol.* **2001**, *18* (1), 127–131.
(38) Konduri, S. D.; Rao, C. N.; Chandrasekar, N.; Tasiou, A.; Mohanam, S.; Kin, Y.; Lakka, S. S.; Dinh, D.; Olivero, W. C.; Gujrati, M.; Foster, D. C.; Kisiel, W.; Rao, J. S. a Novel Function of Tissue Factor Pathway Inhibitor-2 (TFPI-2) in Human Glioma Invasion. *Oncogene* **2001**, *20* (47), 6938–6945.
(39) Yanamandra, N.; Kondraganti, S.; Gondi, C. S.; Gujrati, M.; Olivero, W. C.; Dinh, D. H.; Rao, J. S. Recombinant Adeno-Associated Virus (rAAV) Expressing TFPI-2 Inhibits Invasion, Angiogenesis and Tumor Growth in a Human Glioblastoma Cell Line. *Int. J. Cancer* **2005**, *115* (6), 998–1005.
(40) Sato, N.; Parker, A. R.; Fukushima, N.; Miyagi, Y.; Iacobuzio-Donahue, C. A.; Eshleman, J. R.; Goggins, M. Epigenetic Inactivation of TFPI-2 As a Common Mechanism Associated with Growth and Invasion of Pancreatic Ductal Adenocarcinoma. *Oncogene* **2005**, *24* (5), 850–858.
(41) George, J.; Gondi, C. S.; Dinh, D. H.; Gujrati, M.; Rao, J. S. Restoration of Tissue Factor Pathway Inhibitor-2 in a Human Glioblastoma Cell Line Triggers Caspase-Mediated Pathway and Apoptosis. *Clin. Cancer Res.: Off. J. Am. Assoc. Cancer Res.* **2007**, *13* (12), 3507–3517.
(42) Ran, Y.; Pan, J.; Hu, H.; Zhou, Z.; Sun, L.; Peng, L.; Yu, L.; Liu, J.; Yang, Z. A Novel Role for Tissue Factor Pathway Inhibitor-2 in the Therapy of Human Esophageal Carcinoma. *Human Gene Therapy* **2009**, *20* (1), 41–49.
(43) Konduri, S. D.; Srivenugopal, K. S.; Yanamandra, N.; Dinh, D. H.; Olivero, W. C.; Gujrati, M.; Foster, D. C.; Kisiel, W.; Ali-Osman, F.;

Kondraganti, S.; Lakka, S. S.; Rao, J. S. Promoter Methylation and Silencing of the Tissue Factor Pathway Inhibitor-2 (TFPI-2), a Gene Encoding an Inhibitor of Matrix Metalloproteinases in Human Glioma Cells. *Oncogene* **2003**, *22* (29), 4509–4516.

(44) Rao, C. N.; Segawa, T.; Navari, J. R.; Xu, L.; Srivastava, S.; Moul, J. W.; Phillips, B. Methylation of TFPI-2 Gene Is Not the Sole Cause of Its Silencing. *Int. J. Oncol.* **2003**, *22* (4), 843–848.

(45) Sierko, E.; Wojtukiewicz, M. Z.; Kisiel, W. The Role of Tissue Factor Pathway Inhibitor-2 in Cancer Biology. *Semin. Thromb. Hemost.* **2007**, *33* (7), 653–659.

(46) Steiner, F. A.; Hong, J. A.; Fischette, M. R.; Beer, D. G.; Guo, Z. S.; Chen, G. A.; Weiser, T. S.; Kassis, E. S.; Nguyen, D. M.; Lee, S.; Trepel, J. B.; Schrump, D. S. Sequential 5-Aza 2′-Deoxycytidine/Depsipeptide FK228 Treatment Induces Tissue Factor Pathway Inhibitor 2 (TFPI-2) Expression in Cancer Cells. *Oncogene* **2005**, *24* (14), 2386–2397.

RESEARCH ARTICLE

N-Terminal methylation of proteasome subunit Rpt1 in yeast

Yayoi Kimura, Yoichi Kurata, Akiyo Ishikawa, Akiko Okayama, Masahiro Kamita and Hisashi Hirano

Graduate School of Medical Life Science and Advanced Medical Research Center, Yokohama City University, Yokohama, Japan

Received: May 24, 2013
Revised: August 21, 2013
Accepted: August 28, 2013

The 26S proteasome is a multicatalytic protease complex that degrades ubiquitinated proteins in eukaryotic cells. It consists of a proteolytic core (the 20S proteasome) as well as regulatory particles, which contain six ATPase (Rpt) subunits involved in unfolding and translocation of substrates to the catalytic chamber of the 20S proteasome. In this study, we used MS to analyze the N-terminal modifications of the yeast Rpt1 subunit, which contains the N-terminal recognition sequence for N-methyltransferase. Our results revealed that following the removal of the initiation Met residue of yeast Rpt1, the N-terminal Pro residue is either unmodified, monomethylated, or di-methylated, and that this N-methylation has not been conserved throughout evolution. In order to gain a better understanding of the possible function(s) of the Pro-Lys (PK) sequence at positions 3 and 4 of yeast Rpt1, we generated mutant strains expressing an Rpt1 allele that lacks this sequence. The absence of the PK sequence abolished N-methylation, decreased cell growth, and increased sensitivity to stress. Our data suggest that N-methylation of Rpt1 and/or its PK sequence might be important in cell growth or stress tolerance in yeast.

Keywords:
Cell biology / MS / N-Methylation / Proteasome



Additional supporting information may be found in the online version of this article at the publisher's web-site

1 Introduction

N-terminal methylation, referred to as N-methylation, is a covalent modification of proteins. Several bacterial and eukaryotic proteins are N-methylated, e.g. ribosomal proteins, histone H2B, and regulator of chromosome condensation 1 (RCC1) [1–3]. The phenotype of an N-methylation–defective mutant of human RCC1 reveals that this modification is essential for RCC1's affinity to chromatin and proper mitotic chromosomal segregation [4]. Additionally, N-methylation of *Drosophila* H2B is not only regulated by several external signals such as proliferative or physiological stress, but also changes over the course of fly development [5]. However, the biological significance of N-methylation is known in only a few cases. Recently, the genes *TAE1* and *NTMT1*, which encode N-methyltransferases that catalyze the N-terminal modification of protein substrates, were identified in *Saccharomyces cerevisiae* and human, respectively [2, 4]. N-methyltransferase specifically recognizes the N-terminal Pro-Lys sequence at positions 3 and 4 and selectively mono-, di-, or tri-methylates the amino acid at the N-terminus following removal of the initiation Met.

The ubiquitin-proteasome system is the major ATP-dependent protein degradation machinery in the cell. This system maintains a dynamic equilibrium of proteins and prevents accumulation of damaged and misfolded proteins [6–8]. Ubiquitinated proteins are degraded by the 26S proteasome in an ATP-dependent manner. The 26S proteasome contains a proteolytic core (the 20S proteasome) and its 19S regulatory

Correspondence: Dr. Hisashi Hirano, Graduate School of Medical Life Science and Advanced Medical Research Center, Yokohama City University, 3-9 Fukuura, Kanazawa-ku, Yokohama, Kanagawa 236-0004, Japan
E-mail: hirano@yokohama-cu.ac.jp
Fax: +81-45-787-2787

Abbreviations: RCC1, regulator of chromosome condensation 1; **SC**, synthetic complete; **TEV**, tobacco etch virus

© 2013 WILEY-VCH Verlag GmbH & Co. KGaA, Weinheim

particle (19S RP). The 20S proteasome, which is composed of 14 different subunits, is a multicatalytic protease complex that sequesters the proteolytic active site facing the interior space of the catalytic chamber. In yeast, the 19S RP consists of six different homologous ATPase (Rpt) subunits and at least 13 non-ATPase (Rpn) subunits, and this particle binds one or both ends of the 20S proteasome [8]. The 19S RP is responsible for binding poly-ubiquitin chains, the release of ubiquitin moieties, unfolding of attached substrate proteins, and translocation of substrates into the catalytic chamber of the 20S proteasome. The Rpt subunits form a heterohexameric ring, arranged in the order Rpt1-Rpt2-Rpt6-Rpt3-Rpt4-Rpt5, and are required for unfolding of substrates and opening of the α-ring channel of the 20S proteasome [8, 9].

We previously characterized the N-terminal modifications of the six Rpt subunits of the yeast 26S proteasome [10, 11]. According to our studies in yeast, Rpt2 is partially N-myristoylated, and Rpt3, Rpt4, Rpt5, and Rpt6 are N-acetylated. Previous MS analysis also indicated that following the removal of the initiation Met, the N-terminal Pro residue of Rpt1 is unmodified; however, the N-terminal sequence could not be determined by the Edman degradation method [11]. In light of the discovery of N-methyltransferase and the fact that yeast Rpt1 contains this enzyme's N-terminal recognition motif (Met-Pro-Pro-Lys), Rpt1 must be considered a candidate for N-terminal methylation.

Therefore, in this study we attempted to further analyze the N-terminal modifications of the yeast Rpt1 subunit, using MS. We found that the N-terminal Pro residue can be unmodified, mono-methylated, or di-methylated, and that this N-terminal modification is not conserved throughout evolution. Furthermore, we showed that the absence of the Pro-Lys (PK) sequence at positions 3 and 4 of Rpt1 abolished methylation at the N-terminus, decreased cell growth on YPD medium, and increased sensitivity to canavanine and hydrogen peroxide.

2 Materials and methods

2.1 Yeast strains and medium

Strain SDL66 (*MATa lys2–801 leu2–3, 2–112 ura3–52 his3-Δ200 trp1–1 rpn11::RPN11-TEVProA[HIS3]*) was used as the wild-type strain [12]. The coding sequence of Rpt1, including 420 bp prior to the start codon and 290 bp following the termination codon, was cloned into vector pRS306 to create the plasmid pRS306-RPT1. To obtain an *RPT1* allele encoding a protein lacking the N-terminal PK sequence, pRS306-RPT1 was amplified by PCR using the following primers: 5′-CAGAAGACTGGGAAAAATACAAGGCAC-3′ (forward) and 5′-GCATTCCGTATAGTTCCTAACTTCCTTG-3′ (reverse). The SDL66-derived mutant strain expressing Rpt1 without the N-terminal PK sequence was created by chromosomal integration of inverse PCR-generated disruption cassettes via homologous recombination. All yeast cultures were grown at 30°C. YPD media consisted of 1% w/v yeast extract, 2% w/v Bacto Peptone, and 2% w/v glucose. Synthetic complete (SC) media consisted of 0.67% w/v Difco yeast nitrogen base supplemented with amino acids, uracil, and 2% w/v glucose. Uracil was omitted where necessary for plasmid selections, and arginine was omitted from medium supplemented with canavanine. For tenfold serial-dilution spot assays, freshly grown yeast colonies were suspended in water at an OD (600 nm) of 0.1, and then spotted on a YPD plate, a YPD plate containing 1 mM hydrogen peroxide (Wako, Tokyo, Japan) an SC media plate, or an SC media plate containing 0.5 μg/mL canavanine (Sigma, Madison, WI, USA). Spotted plates were incubated for 38–62 h.

2.2 Purification of the yeast 26S proteasome

SDL66 cells were cultured in YPD medium and grown to late logarithmic phase, ~3 A_{600} U/mL for the wild-type strain or ~2 A_{600} U/mL for the mutant strain. The yeast cells were harvested by centrifugation and washed twice with deionized water. The 26S proteasome was purified as described by Leggett et al. [12], with slight modifications as described below. Briefly, yeast cells were disrupted by homogenization in a Bead-Beater (BioSpec Products, Bartlesville, OK, USA) in 50 mM phosphate buffer, pH 7.5, containing 4 mM ATP, 10 mM $MgCl_2$, 1 mM DTT, 1 mM EDTA, 10% v/v glycerol, and 1 μg/mL leupeptin, and then total cell lysate was obtained by centrifugation at 20 000 × *g* for 30 min at 4°C, followed by filtration using a 0.45-μm membrane filter. Lysates were stored at −80°C until further use. To purify 26S proteasomes, total cell lysates were incubated for 1 h at 4°C with IgG resin (GE Healthcare, Little Chalfont, UK). After incubation, the resin was washed with wash buffer (50 mM phosphate buffer, pH 7.5, containing 1 mM ATP, 5 mM $MgCl_2$, 1 mM DTT, and 50 mM NaCl), followed by TEV (tobacco etch virus) protease buffer (50 mM phosphate buffer, pH 7.5, containing 1 mM ATP, 5 mM $MgCl_2$, 1 mM DTT, and 1 mM EDTA). To elute proteasomes, the resin was incubated with TEV protease buffer containing TEV protease (Promega, WI, USA) for 1 h at room temperature. Purified proteasomes were stored at −80°C in TEV protease buffer containing 10% v/v glycerol.

2.3 Protein electrophoresis

SDS-PAGE was performed using polyacrylamide slab gels purchased from Wako followed by CBB staining (Life Technologies, Carlsbad, CA, USA) or Oriole Fluorescent Gel Stain (Bio-Rad Laboratories, Hercules, CA, USA) for protein detection, or by electroblotting onto PVDF membranes for immunoblotting analysis. For 2DE, protein was diluted in 2DE rehydration buffer (7M urea, 2M thiourea, 4% w/v CHAPS, 20 mM DTT, and 0.5% v/v IPG buffer, pH 3–10NL [GE Healthcare]) and then applied to an IPG dry strip gel (7 cm,

© 2013 WILEY-VCH Verlag GmbH & Co. KGaA, Weinheim

pH 3–10NL [GE Healthcare]) by in-gel rehydration for 16 h at room temperature. IEF in the first dimension was performed using the ZOOM IPGRunner system (Life Technologies). For the second dimension, a homemade 10% w/v polyacrylamide gel was used. After electrophoresis, the separated proteins were stained with CBB.

2.4 Immunoprecipitation of the human Rpt1 subunit

HEK293 cells were lysed in human-cell lysis buffer (50 mM Tris-HCl, pH 7.5, containing 50 mM NaCl, 4 mM ATP, 10 mM $MgCl_2$, 1 mM DTT, 1 mM EDTA, and 10% v/v glycerol) containing 0.5% v/v NP-40, and then centrifuged. To purify human Rpt1, the supernatant was diluted five-fold in human-cell lysis buffer and then incubated with anti–α2 subunit antibody (PW8105, Enzo Life Sciences, Farmingdale, NY, USA) bound to protein G–Sepharose (GE Healthcare) for 16 h at 4°C for immunoprecipitation. After washing the protein G–Sepharose/antibody complexes, the immunoprecipitated proteasomes were eluted with 1 M glycine buffer and separated by SDS-PAGE, followed by CBB staining.

2.5 MS analysis

Proteins were excised from CBB-stained gels, destained, and subjected to in-gel digestion overnight at 37°C with 5 ng/μL endoproteinase Glu-C (Sigma) or 12.5 ng/μL trypsin (Promega) in 25 mM ammonium bicarbonate. For analysis on a MALDI-TOF/TOF MS (4800 Proteomics Analyzer, AB SCIEX, Foster City, CA, USA), the resulting peptides were desalted using a ZipTip-C18μ (Millipore, Bedford, MA, USA) and then eluted directly onto a target plate with matrix solution containing 4 mg/mL CHCA (Sigma). For protein identification, mass spectra were acquired over a mass range of *m/z* 800–4000, and a job-wide interpretation method allowed the 20 highest intensity peptides of each spot to be sequenced in MS/MS mode. Peak lists were created using the "Peak to MASCOT" tool of the 4000 Series Explorer Software version 3.5.1 (AB SCIEX). To identify the sequence of the yeast Rpt1 subunit, the tryptic digests were desalted using C18 membrane filters, and then analyzed on a nano-LC/tripleTOF MS (TripleTOF 5600 system, AB SCIEX). In that case, peak lists were created using Analyst version 1.6TF (AB SCIEX). The obtained MS and tandem-MS data were searched against the *S. cerevisiae* protein sequences in the Uniprot/Swiss-Prot database (version Jan 2013) using the MASCOT software, version 2.4.1 (Matrix Science, London, UK). The search parameters were as follows: three missed cleavages permitted; variable modifications: N-methylation, N-dimethylation, oxidation of methionine, and propionamidation of cysteine; peptide mass tolerance for MS data, ±15 ppm (MALDI-TOF/TOF MS) or ±0.05 Da (nano-LC/tripleTOF MS); and fragment mass tolerance, ±0.3 Da (MALDI-TOF/TOF MS) or ±0.1 Da (nano-LC/tripleTOF MS). For evaluation of database-search results using MASCOT, "bold red" peptides with a peptide score ≥ 25 were considered as evaluation peptides. Proteins that contained at least two evaluation peptides and had a protein score ≥ 50 were accepted as positive identifications in MALDI-TOF/TOF MS.

2.6 Immunoblotting analysis

The following antibodies were used for immunoblotting: anti–19S RP subunit Rpt1 (S7) (PW8165), anti–20S proteasome subunit α7 (PW8110), and HRP-conjugated anti-ubiquitin (FK2) antibody (PW0150) (Enzo Life Sciences). Anti-α7 antibody was the useful antibody that can detect the proteasome subunit in both the purified 26S proteasomes and total cell lysates. These antibodies were visualized with HRP-conjugated primary or secondary antibodies using Chemi-Lumi One Super (Nacalai Tesque, Kyoto, Japan) on an LAS 4000 mini luminescence image analyzer (GE Healthcare).

3 Results

3.1 N-terminal methylation of the yeast Rpt1 subunit

In order to determine the N-terminal modifications of yeast Rpt1, we purified 26S proteasomes from the wild-type strain. In the strain we used, the Rpn11 subunit is tagged with TEV protease–cleavable protein A, allowing purification by binding to IgG resin. Purified proteasomes were separated by SDS-PAGE, and subsequently each subunit band was detected by CBB staining. For protein identification, each band was digested with trypsin and then analyzed by MALDI-TOF/TOF MS. By this method, we identified the 25 proteasome subunits that constitute the yeast 26S proteasome (Fig. 3A and Supporting Information Table 1). To confirm N-terminal modification of Rpt1, we analyzed the N-terminal peptide of Rpt1 after digestion with endoproteinase Glu-C, which was expected to generate an N-terminal peptide appropriately sized for analysis by MALDI-TOF/TOF MS. The MS analysis detected five peptides (*m/z* 914.4, 928.4, 3553.7, 3567.7, and 3581.7), which were identical to the theoretical mass of the N-terminal peptide (Fig. 1A, Supporting Information Fig. 1A and Supporting Information Table 2). Tandem mass spectra of signals at *m/z* 914.4 and *m/z* 928.4 enabled us to precisely assign the N-terminal peptides (PPKEDWE) mono- and di-methylated at the Pro residue that is N-terminal following removal of the initiation Met (Supporting Information Fig. 1B). Tandem mass spectra of the signals at *m/z* 3553.7, *m/z* 3567.7, and *m/z* 3581.7 revealed sequences corresponding to the unmodified, mono- and di-methylated N-terminal peptide of yeast Rpt1 (PPKEDWEKYKAPLEDDD-KKPDDDKIVPLTE); (Fig. 1B and Supporting Information Fig. 1B). Thus, the MS analysis indicated that the N-terminus

© 2013 WILEY-VCH Verlag GmbH & Co. KGaA, Weinheim

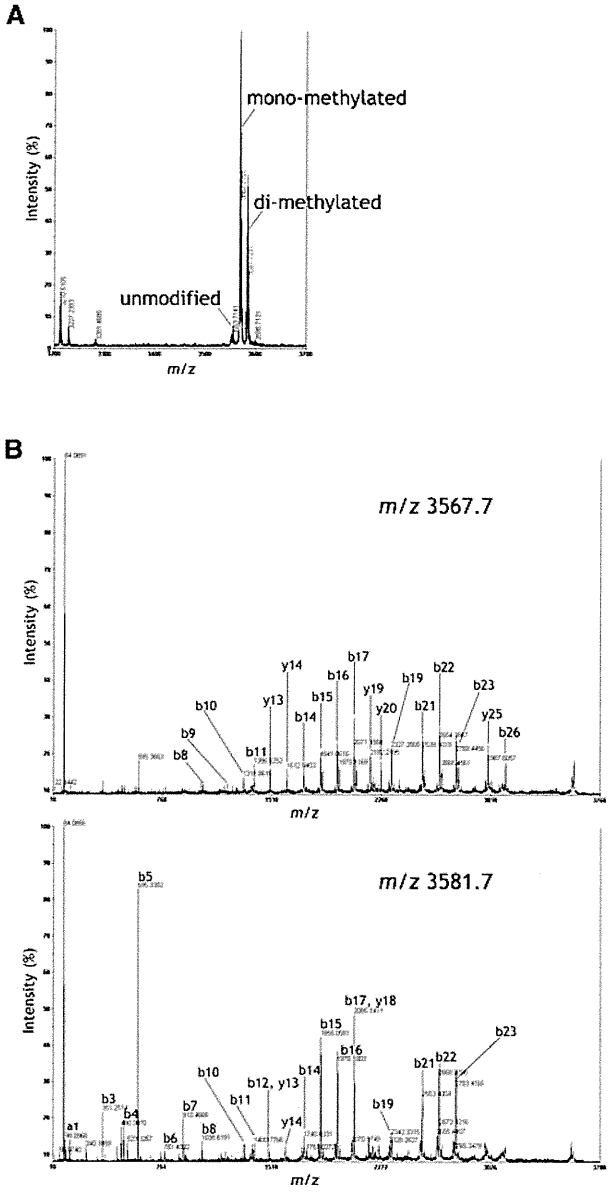

Figure 1. Identification of the N-terminal modification of the Rpt1 subunit from a wild-type yeast strain. Mass spectra (A, *m/z* 3200–3700) and tandem mass spectra (B) from endoproteinase Glu-C digests of the Rpt1 subunit from the wild-type strain. The Rpt1 subunit was separated by SDS-PAGE followed by CBB staining, and then subjected to in-gel digestion with endoproteinase Glu-C. The resulting digests were analyzed by MALDI-TOF/TOF MS. Fragment ions of the a-, b-, and y-series identified in the tandem mass spectra from each peptide are shown in the figure. Tandem mass spectra of the signals at *m/z* 3567.7 and *m/z* 3581.7 revealed sequences corresponding to the N-terminal peptide (PPKEDWEKYKAPLEDDDKKPDDDKIVPLTE) mono- and di-methylated at the Pro residue that is N-terminal following removal of the initiation Met. Tandem mass spectrum of the signal at *m/z* 3553.7, which is identical to the theoretical mass of the unmodified N-terminal peptide (PPKEDWEKYKAPLEDDDKKPDDDKIVPLTE), indicated in Supporting Information Fig. 1B.

of yeast Rpt1 has three forms: unmodified, mono-methylated, and di-methylated at the Pro residue that is N-terminal following the removal of the initiation Met. In our previous study, we concluded that the N-terminal Pro of yeast Rpt1 subunit is unmodified, because only acetylation was set as a variable N-terminal modification in the database-search parameters of the MASCOT software [11]. When variable N-methylation was set as a MASCOT database-search parameter, the N-terminal mono- or di-methylated peptide could be detected in the previous MS and tandem-MS data. Therefore, we concluded that the N-terminal Met of the yeast Rpt1 subunit precursor polypeptide is cotranslationally removed to generate the mature protein, and that the resulting N-terminal Pro is unmodified, mono-methylated, or di-methylated.

Multiple alignment of amino-acid sequences of Rpt1 subunit from several species indicated that the PK sequence, which is the N-terminal recognition sequence for N-methyltransferase, was not conserved during the course of evolution and is instead unique to yeast (Fig. 2A). To characterize the N-terminal modification of the human Rpt1 subunit, which has no N-terminal recognition sequence for N-methyltransferase, we analyzed tryptic digests derived from human Rpt1 using MALDI-TOF/TOF MS. The mass spectra and tandem mass spectra of the N-terminal peptides (*m/z* 1034.4 and *m/z* 1162.5) derived from human Rpt1 revealed that the initiation Met of the precursor was removed cotranslationally, but the N-terminal Pro was unmodified (Fig. 2B, Supporting Information Fig. 1C and Supporting Information Table 2). This finding was consistent with data from a previous MS analysis [13]. From these results, we conclude that N-methylation of Rpt1 is a yeast-specific modification.

3.2 Characteristics of Rpt1 lacking the N-terminal PK sequence

In order to gain a better understanding of the possible role(s) of the N-terminal PK sequence of yeast Rpt1, we generated a mutant strain expressing an Rpt1 allele that lacks the unique Pro and Lys residues at positions 3 and 4, and then purified 26S proteasomes from wild-type and PK-deletion cells. When purified proteasomes were separated by SDS-PAGE followed by CBB staining or immunoblotting analysis to detect Rpt1 or 20S proteasome α7 subunit, we observed a mobility shift in the Rpt1 subunit from the PK-deletion strain, relative to that of the wild-type strain; no mobility shift was detected in proteasome subunits containing α7 (Fig. 3A and B). Shotgun MS analysis of tryptic digests from Rpt1 expressed in the wild-type and PK-deletion strain by nano-LC/tripleTOF MS could identify 78% of the sequence, including N-terminal and C-terminal peptides, but there were no differences between the amino-acid sequences detected in each strain (data not shown). To more precisely characterize PK-deleted Rpt1, we used 2DE, in which the first dimension was isoelectric focusing (IPG) and the second dimension was SDS-PAGE. After

© 2013 WILEY-VCH Verlag GmbH & Co. KGaA, Weinheim

A

```
Oryza sativa              ----------MAPEPE----DDIM-NEKNPRPLDEDDIALLK
Spinacia oleracea         ----------MAIEHE----DDLK-DEKNPRPLDEDDIALLK
Arabidopsis thaliana      ----------MVRDIE----DEIR-DEKNPRPLDEDDIALLK
Homo sapiens              MP--DYLGADQRKTKE----DEK--DDKPIRALDEGDIALLK
Bos taurus                MP--DYLGADQRKTKE----DEK--DDKPIRALDEGDIALLK
Mus musculus              MP--DYLGADQRKTKE----EEK--DDKPIRALDEGDIALLK
Xenopus laevis            MP--DYLGADQRKTKE----EEK--EDKPIRSLDEGDIALLK
Caenorhabditis elegan     MP--DHLGDDMRKTKK----DDTKEEEKNFQALDEGDIAVLK
Penicillium marneffei     MP--SATGSNWEKYQKNFADDEIP--EKKITPLTDEDIQVLK
Aspergillus oryzae        MP--SATGENWEKYKKNFADDEEP--EKKITPLTESDIQVLK
Schizosaccharomyces pombe MPPK----EDWEKYQKPVDTEEEN--DKNPPPLDEGDIELLK
Saccharomyces cerevisiae  MPPK----EDWEKYKAPLEDDDKKPDDDKIVPLTEGDIQVLK
                            * *
```

B

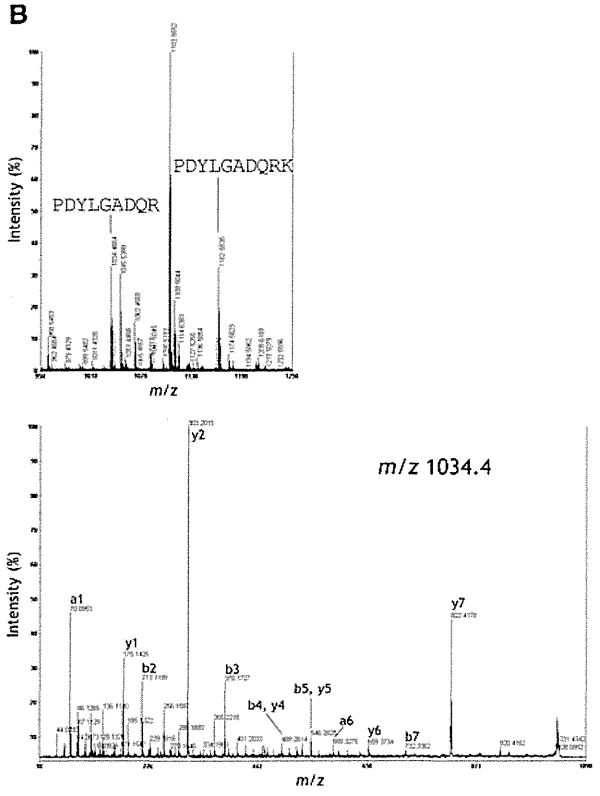

Figure 2. Conservation of the N-terminal sequence and methylation of the Rpt1 subunit. (A) Alignment of the N-terminal region of the Rpt1 subunit. Multiple sequence alignment of amino-acid sequences from several diverse species was performed using ClustalX. Asterisks indicate an N-terminal recognition motif for N-methyltransferase. (B) Mass spectra (upper panel, *m/z* 950–1250) and tandem mass spectra (bottom panel) from tryptic digests of the human Rpt1 subunit. The human Rpt1 subunit was separated by SDS-PAGE followed by CBB staining, and then subjected to in-gel digestion with trypsin. The resulting digests were analyzed using MALDI-TOF/TOF MS. Fragment ions of the a-, b-, and y-series identified in the tandem mass spectra from each peptide are shown in the figure. Tandem mass spectrum of the signal at *m/z* 1034.4 revealed a sequence corresponding to the unmodified N-terminal peptide (PDYLGADQR) of human Rpt1 without the initiation Met. Tandem mass spectrum of the signal at *m/z* 1162.5, which is identical to the theoretical mass of the other unmodified N-terminal peptide (PDYLGADQRK) of human Rpt1, indicated in Supporting Information Fig. 1C.

the 2DE, proteasome subunits were detected by CBB staining. These experiments revealed a subtle shift in the acidic direction of the isoelectric point of PK-deleted Rpt1, relative to that of wild-type Rpt1 (Fig. 3C). It is possible that this change in the isoelectric point contributed to the SDS-PAGE mobility shift of PK-deleted Rpt1. In order to investigate the N-terminal modification of the Rpt1 subunit, we subjected the excised band to in-gel digestion with endoproteinase Glu-C, and analyzed digests of PK-deleted Rpt1 by MALDI-TOF/TOF-MS. The MS analysis detected a peptide (*m/z* 3328.5), identical to the theoretical mass of the PK-deleted N-terminal peptide generated by endoproteinase Glu-C from Rpt1 following loss of the N-terminal Met (Fig. 3D upper panel). We also found a peptide (*m/z* 3459.6) corresponding to the PK-deleted N-terminal peptide with the initiation Met residue. The tandem mass spectra of these peptides enabled us to precisely assign the exact peptide (Fig. 3D bottom panel, Supporting Information Fig. 1D and Supporting Information Table 2). However, in the PK-deleted strain, the N-methylated peptides could not be detected by MS analysis, whereas a signal in MS of the methylated and di-methylated peptides showed very high intensity compared to that of the unmodified peptide in the wild type (Fig. 1A and 3D upper panel). Therefore, our data indicate that the PK sequence is critical for the isoelectric point and N-methylation of yeast Rpt1.

3.3 Characteristics of the yeast PK-deletion strain

In order to determine the importance of the unique PK sequence at the N-terminus of the yeast Rpt1 subunit, we investigated the cell growth of the mutant strain bearing the PK-deleted Rpt1 subunit in YPD medium at 30°C. The mutant strain grew more slowly: doubling times were ~1.9 h for the wild-type strain and 2.8 h for the PK-deletion strain (Fig. 4A). Next, we studied the stress tolerance of the PK-deletion strain using tenfold serial-dilution spot assays on YPD plates containing hydrogen peroxide or SC media plates containing canavanine, both at 30°C. Hydrogen peroxide is a powerful oxidant; proteasome subunits can themselves be targets for oxidative modification, which can reduce the activity of the 26S proteasome [14]. Canavanine is an arginine analog whose toxicity is typically enhanced in proteolysis-deficient mutants. The PK-deletion strain grew more slowly under both stress conditions than on control plates, whereas the wild-type strain grew equally well under stress and control conditions (Fig. 4B). These results suggest that methylation and/or the N-terminal PK sequence of Rpt1 is important for cell growth and tolerance to some stresses in yeast. However, no significant difference was observed between the wild-type and PK-deletion strains when total cell lysates were subjected to SDS-PAGE followed by CBB staining or immunoblotting analysis for detection of 20S proteasome α7 subunit and ubiquitin, by which the accumulation of poly-ubiquitinated proteins due to deficient proteasome activity can be confirmed (Fig. 4C and D). Thus, it remains unknown how the absence

© 2013 WILEY-VCH Verlag GmbH & Co. KGaA, Weinheim

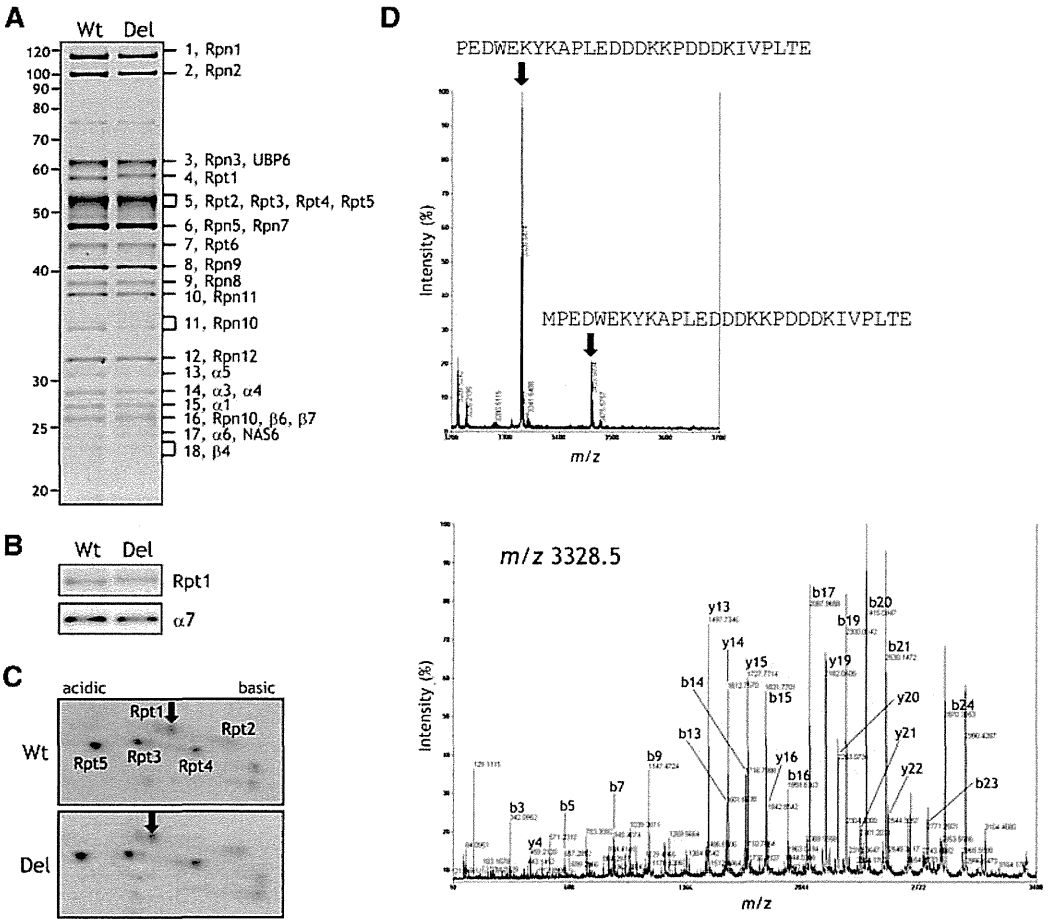

Figure 3. Characteristics of the yeast Rpt1 subunit lacking the N-terminal PK sequence. (A) SDS-PAGE gel image of the 26S proteasome from the wild-type and PK-deletion strains. Purified 26S proteasomes were separated by SDS-PAGE followed by CBB staining. Each band was excised from the gel and identified by MS analysis using MALDI-TOF/TOF MS after in-gel digestion with trypsin. Band numbers correspond to those in Supporting Information Table 1. (B) The Rpt1 and α7 subunits of the purified 26S proteasome from the wild-type and PK-deletion strains were detected by immunoblotting analysis with the indicated antibody. (C) Expanded CBB-stained 2DE gel image of purified 26S proteasomes from the wild-type and PK-deletion strains. (D) Mass spectra (upper panel, *m/z* 3200–3700) and tandem mass spectra (bottom panel) from endoproteinase Glu-C digests of PK-deleted Rpt1. The Rpt1 subunit from the PK-deletion strain was separated by SDS-PAGE followed by CBB staining and in-gel digestion with endoproteinase Glu-C. The resulting digests were analyzed by MALDI-TOF/TOF MS. Fragment ions of the b- and y-series identified in the tandem mass spectra from each peptide are shown in the figure. Tandem mass spectrum of the signal at *m/z* 3328.5 revealed a sequence corresponding to the unmodified N-terminal peptide (PEDWEKYKAPLEDDDKKPDDDKIVPLTE) without the initiation Met and PK sequence. Tandem mass spectrum of the signal at *m/z* 3459.6, which is identical to the theoretical mass of the unmodified N-terminal peptide (MPEDWEKYKAPLEDDDKKPDDDKIVPLTE) with the initiation Met but without the PK sequence, indicated in Supporting Information Fig. 1D. "Wt" and "Del" indicate the wild-type and PK-deletion strains, respectively.

of the N-terminal PK sequence of Rpt1 affected the phenotypes of the PK-deletion strain.

4 Discussion

A major focus in proteomics is analysis of the co- and post-translational modifications of proteins. In human, mouse, and yeast proteasome, extensive mapping of co- and post-translational modifications has been carried out, and several protein modifications, including oxidative modifications, ubiquitination, N-acetylation, N-myristoylation, phosphorylation, and glycosylation, have been reported [10, 11, 13, 15]. These modifications play roles in regulating proteasome stability, assembly, and/or activity. In a previous study, we concluded from MS analysis that the N-terminal Pro of yeast Rpt1 is unmodified [11]. Subsequently, the discovery of the N-methyltransferase revealed that the N-terminal sequence of Rpt1, Met-Pro-Pro-Lys-, is an N-terminal recognition motif of N-methyltransferase; therefore, Rpt1 had to be considered as a candidate for methylation. In this study, we showed that

© 2013 WILEY-VCH Verlag GmbH & Co. KGaA, Weinheim

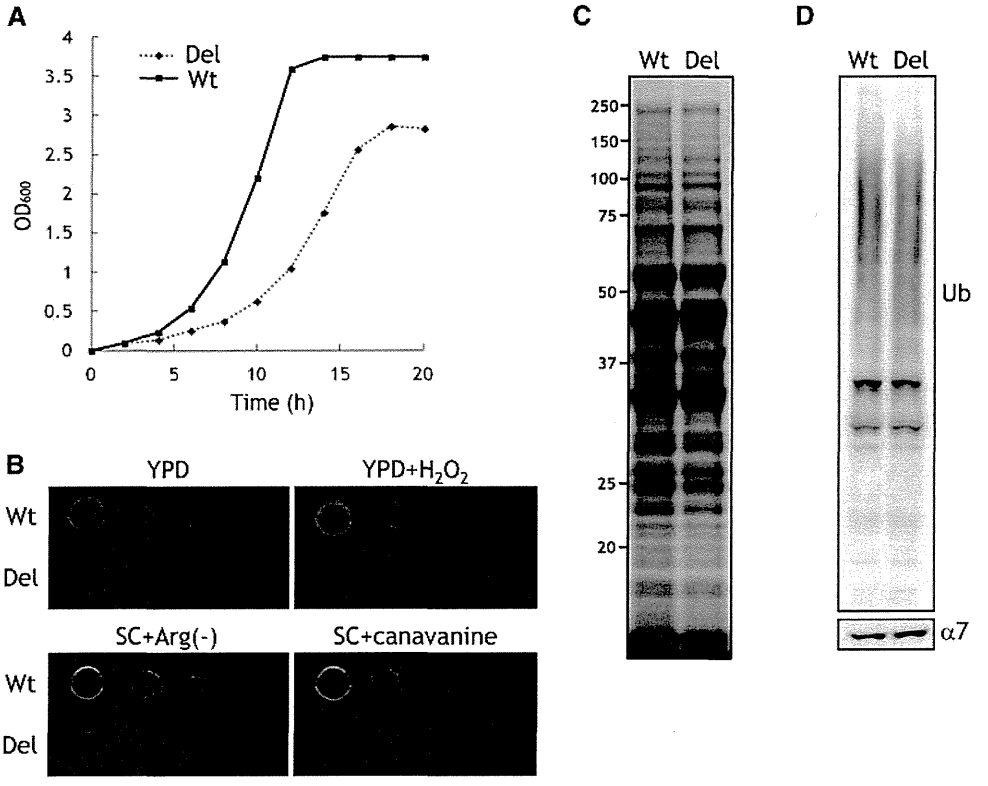

Figure 4. Phenotypes of a yeast strain expressing an Rpt1 subunit lacking the N-terminal PK sequence. (A) Growth curves of the wild-type and PK-deletion strains. Each strain was cultured in YPD at 30°C, and culture turbidity was measured at 600 nm. (B) Effect of each stress on growth of the wild-type and PK-deletion strains. Details of the procedure for the tenfold serial-dilution spot assay are described in Section 2. (C) SDS-PAGE gel image of total cell lysate from the wild-type and PK-deletion strains. The total cell lysates were separated by SDS-PAGE followed by CBB straining. (D) Ubiquitin-conjugated protein and the α7 subunit from total cell lysates from the wild-type and PK-deletion strains detected by immunoblotting analysis with the indicated antibody. "Wt" and "Del" indicate the wild-type and PK-deletion strains, respectively.

the N-terminus of yeast Rpt1 exists in three forms: unmodified, mono-methylated, and di-methylated at the Pro residue that is at the N-terminus following removal of the initiation Met.

MS-based peptide sequencing is one of the most reliable techniques for identification of protein modifications in a high-throughput manner. Experimental indications regarding protein modifications are based on results from database-search engines such as the MASCOT (Matrix Science) and ProteinPilot (AB Sciex) software, which are a widely used in the identification of proteins. MASCOT is a commercially available database-search engine that accepts raw data from several different mass spectrometers [16]. To characterize protein modifications from primary protein-sequence databases using MASCOT, the search parameter(s) must be generally entered as "fixed" or "variable" modifications. It is difficult to detect peptide with a modification without information regarding that modification. Indeed, in the previous study, we did not consider N-methylation as a potential N-terminal modification of yeast Rpt1. ProteinPilot, in which the Paragon algorithm is used, is a database-search engine designed to process tandem-MS data from instruments from AB Sciex. ProteinPilot allows simultaneous search for hundreds of biological and other modifications, genetic variants, and unexpected cleavages that may occur, depending on their frequencies [17]. However, N-methylation is a rare modification in eukaryotic proteins, and the probability for N-methylation in ProteinPilot is low relative to those of other modifications, e.g. N-acetylation, which is one of the most common modifications of the N-terminus and occurs on approximately 57% of yeast proteins. Hence, the ProteinPilot software also failed to detect the N-terminal Rpt1 peptide containing methylated Pro in our previous MS data. These programs cannot easily detect unknown minor modification of peptides. Therefore, information about the recognition motifs of modification enzyme will also be important for identification of proteins with rare modifications, as demonstrated by the MS analysis in this study.

Our data also indicated that the PK sequence, which is an N-terminal recognition sequence for N-methyltranseferase, was critical for N-methylation of yeast Rpt1. In addition, the PK-deletion strain exhibited decreased cell growth and increased sensitivity to oxidant and canavanine stress relative to the wild-type strain. These results demonstrated the involvement of the N-terminal PK sequence of yeast Rpt1 in N-methylation, cell growth, and stress tolerance, suggesting that the N-terminus is important in determining the protein's function. However, it is not clear whether loss of N-methylation of yeast Rpt1 directly affects the cellular phenotype. Although the lack of N-methylation does not change protein charge, the absence of the PK sequence does result in loss of positive charge at the N-terminus. It is possible that this loss of N-terminal positive charge contributes to the phenotypes of a strain expressing Rpt1 without the PK sequence. Unfortunately, definitive evidence regarding the cause of decreased cell growth and increased sensitivity to stress

© 2013 WILEY-VCH Verlag GmbH & Co. KGaA, Weinheim

tolerance in the PK-deletion strain, such as a demonstrable change in proteasome activity, is not yet available.

Each of the proteasome ATPase subunits is highly evolutionarily conserved: sequence identities range from 66–76% between the yeast and human homologs [18]. As for N-terminal modification of the proteasome ATPase subunits, N-myristoylation of the Rpt2 and N-acetylation of the Rpt3, Rpt4, Rpt5, and Rpt6 are conserved between yeast and human [10, 13]. However, neither N-methylation nor the N-terminal PK sequence of Rpt1 is conserved throughout evolution. Similarly, RCC1 is N-methylated in human but not *Drosophila*, whereas H2B is N-methylated in *Drosophila* but not human [5]. It is surprising that the evolutionary conservation of N-methylation and the N-terminal recognition sequence for N-methyltransferase is low. On the other hand, there are also proteins in which the N-terminal PK sequence has been conserved, e.g. 40S ribosomal protein S25 (RPS25) and 60S ribosomal protein L12 (RPL12), which are N-dimethylated in yeast [2]. In addition, the degree of N-methylation of proteins changes under specific conditions. The biological significance of methylation and/or the N-terminal PK sequence may therefore differ in each protein or species due to the amino-acid sequences of other regions and/or conformations of protein.

The authors thank Dr. Daniel Finley for providing SDL66 cells. This work was supported by the Special Coordination Fund for Promoting Science and Technology, "Creation and Innovation Centers for Advanced Interdisciplinary Research Areas."

The authors have declared no conflict of interest.

5 References

[1] Stock, A., Clarke, S., Clarke, C., Stock, J., N-terminal methylation of proteins: structure, function and specificity. *FEBS Lett.* 1987, *220*, 8–14.

[2] Webb, K. J., Lipson, R. S., Al-Hadid, Q., Whitelegge, J. P., Clarke, S. G., Identification of protein *N*-terminal methyltransferases in yeast and humans. *Biochemistry* 2010, *49*, 5225–5235.

[3] Wang, Z. Y., Shimonaga, M., Kobayashi, M., Nozawa, T., N-terminal methylation of the core light-harvesting complex in purple photosynthetic bacteria. *FEBS Lett.* 2002, *519*, 164–168.

[4] Tooley, C. E., Petkowski, J. J., Muratore-Schroeder, T. L., Balsbaugh, J. L. et al., NRMT is an alpha-*N*-methyltransferase that methylates RCC1 and retinoblastoma protein. *Nature* 2010, *466*, 1125–1128.

[5] Villar-Garea, A., Forne, I., Vetter, I., Kremmer, E. et al., Developmental regulation of *N*-terminal H2B methylation in *Drosophila melanogaster*. *Nucleic Acids Res.* 2012, *40*, 1536–1549.

[6] Finley, D., Recognition and processing of ubiquitin-protein conjugates by the proteasome. *Annu. Rev. Biochem.* 2009, *78*, 477–513.

[7] Ravid, T., Hochstrasser, M., Diversity of degradation signals in the ubiquitin-proteasome system. *Nat. Rev. Mol. Cell Biol.* 2008, *9*, 679–690.

[8] Tomko Jr, R. J., Hochstrasser, M., Molecular architecture and assembly of the eukaryotic proteasome. *Annu. Rev. Biochem.* 2013, *82*, 415–445.

[9] Tomko Jr, R. J., Funakoshi, M., Schneider, K., Wang, J., Hochstrasser, M., Heterohexameric ring arrangement of the eukaryotic proteasomal ATPases: implications for proteasome structure and assembly. *Mol. Cell* 2010, *38*, 393–403.

[10] Kimura, Y., Saeki, Y., Yokosawa, H., Polevoda, B. et al., *N*-Terminal modifications of the 19S regulatory particle subunits of the yeast proteasome. *Arch. Biochem. Biophys.* 2003, *409*, 341–348.

[11] Kikuchi, J., Iwafune, Y., Akiyama, T., Okayama, A. et al., Co- and post-translational modifications of the 26S proteasome in yeast. *Proteomics* 2010, *10*, 2769–2779.

[12] Leggett, D. S., Glickman, M. H., Finley, D., Purification of proteasomes, proteasome subcomplexes, and proteasome-associated proteins from budding yeast. *Methods Mol. Biol.* 2005, *301*, 57–70.

[13] Wang, X., Chen, C. F., Baker, P. R., Chen, P. L. et al., Mass spectrometric characterization of the affinity-purified human 26S proteasome complex. *Biochemistry* 2007, *46*, 3553–3565.

[14] Ishii, T., Sakurai, T., Usami, H., Uchida, K., Oxidative modification of proteasome: identification of an oxidation-sensitive subunit in 26 S proteasome. *Biochemistry* 2005, *44*, 13893–13901.

[15] Kimura, Y., Takaoka, M., Tanaka, S., Sassa, H. et al., *N*(alpha)-acetylation and proteolytic activity of the yeast 20 S proteasome. *J. Biol. Chem.* 2000, *275*, 4635–4639.

[16] Perkins, D. N., Pappin, D. J., Creasy, D. M., Cottrell, J. S., Probability-based protein identification by searching sequence databases using mass spectrometry data. *Electrophoresis* 1999, *20*, 3551–3567.

[17] Shilov, I. V., Seymour, S. L., Patel, A. A., Loboda, A. et al., The Paragon Algorithm, a next generation search engine that uses sequence temperature values and feature probabilities to identify peptides from tandem mass spectra. *Mol. Cell Proteomics* 2007, *6*, 1638–1655.

[18] Glickman, M. H., Rubin, D. M., Fried, V. A., Finley, D., The regulatory particle of the *Saccharomyces cerevisiae* proteasome. *Mol. Cell Biol.* 1998, *18*, 3149–3162.

© 2013 WILEY-VCH Verlag GmbH & Co. KGaA, Weinheim